https://doi.org/10.5194/bg-2021-123
Preprint. Discussion started: 18 May 2021

Biogeosciences Discussions
Open Access
EGU

Biological production in two contrasted regions of the Mediterranean Sea during the oligotrophic period: An estimate based on the diel cycle of optical properties measured by BGC-Argo profiling floats

Marie Barbieux[1], Julia Uitz[1], Alexandre Mignot[2], Collin Roesler[3], Hervé Claustre[1], Bernard Gentili[1], Vincent Taillandier[1], Fabrizio D'Ortenzio[1], Hubert Loisel[4], Antoine Poteau[1], Edouard Leymarie[1], Christophe Penkerc'h[1], Catherine Schmechtig[5], Annick Bricaud[1]

[1]CNRS and Sorbonne Université, Laboratoire d'Océanographie de Villefranche, LOV, 06230 Villefranche-sur-Mer, France

[2]Mercator Océan, 31520 Ramonville-Saint-Agne, France

[3]Bowdoin College, Earth and Oceanographic Science, Brunswick, Maine 04011, USA

[4]Université Littoral Côte d'Opale, Université Lille, CNRS, Laboratoire d'Océanologie et de Géosciences, 59000 Lille, France

[5]OSU Ecce Terra, UMS 3455, CNRS and Sorbonne Université, Paris 6, 4 place Jussieu, 75252 Paris CEDEX 05, France

Correspondence to: J. Uitz (julia.uitz@imev-mer.fr)

https://doi.org/10.5194/bg-2021-123
Preprint. Discussion started: 18 May 2021


Biogeosciences Discussions

Abstract

This study assesses marine biological production of organic carbon based on the diel variability of bio-optical properties monitored by two BioGeoChemical-Argo (BGC-Argo) floats. Experiments were conducted in two distinct Mediterranean systems, the Northwestern Ligurian Sea and the Central Ionian Sea during summer months. We derived particulate organic carbon (POC) stock and gross community production integrated within the surface, euphotic and subsurface chlorophyll maximum (SCM) layers, using an existing approach applied to diel cycle measurements of the particulate beam attenuation (c_p) and backscattering (b_{bp}) coefficients. The diel cycle of c_p provided a robust proxy for quantifying biological production in both systems; that of b_{bp} was comparatively less robust. Derived primary production estimates vary by a factor of 2 depending upon the choice of the bio-optical relationship that converts the measured optical coefficient to POC, which is thus a critical step to constrain. Our results indicate a substantial, yet variable, contribution to the water column production of the SCM layer (16–42%). In the Ligurian Sea, the SCM is a seasonal feature that behaves as a subsurface biomass maximum (SBM) with the ability to respond to episodic abiotic forcing by increasing production. In contrast, in the Ionian Sea, the SCM is permanent, induced by phytoplankton photoacclimation and contributes moderately to water column production. These results emphasize the strong potential for transmissometers deployed on BGC-Argo profiling floats to quantify non-intrusively *in situ* biological production of organic carbon in the water column of stratified oligotrophic systems with recurring or permanent SCMs, which are widespread features in the global ocean.

https://doi.org/10.5194/bg-2021-123
Preprint. Discussion started: 18 May 2021

1 Introduction

Primary production is an essential component of the global ocean carbon cycle (Field et al. 1998). As a major driver of the biological carbon pump, this biogeochemical process plays a critical role in the regulation of the Earth climate (e.g. Sarmiento & Siegenthaler 1992; Falkowski 2012). Hence, quantifying primary production in the ocean stands as a major challenge in the context of climate change. The balance between gross primary production and community respiration in the ocean determines the trophic status of marine systems, i.e. whether the system acts as a source or a sink of carbon (Williams 1993). This balance depends on the considered region and varies substantially according to spatial and temporal scales (Geider et al. 1997; Duarte & Agusti 1998; del Giorgio & Duarte 2002). It is therefore necessary to develop capabilities not only for assessing primary production on a global scale, but also for characterizing and quantifying the biogeochemical functioning of marine ecosystems at smaller spatial and temporal scales (Serret et al. 1999; González et al. 2001 & 2002).

Traditionally, primary production measurements are based on *in situ* or *in vitro* incubation experiments (i.e. on board the ship, under controlled conditions) coupled with isotopic carbon analysis (Nielsen 1952; Fitzwater et al. 1982; Dandonneau 1993; Barber & Hitling 2002) or measurements of oxygen concentration (Williams & Jenkinson 1982; Williams & Purdie 1991). These methods involve seawater sampling during field campaigns, sample manipulation and subsequent laboratory analyses, which are both time consuming and require strong technical expertise. As a result, the availability of field primary production measurements is relatively limited in terms of spatial and temporal coverage, which hinders the possibility of extrapolation to other systems or to larger space and time scales for modeling purposes.

https://doi.org/10.5194/bg-2021-123
Preprint. Discussion started: 18 May 2021

Bio-optical primary production models coupled with ocean color satellite imagery represent another approach for obtaining primary production estimates (Morel 1991; Longhurst et al. 1995; Antoine et al. 1996; Behrenfeld et al. 2002). Such models are extremely valuable for assessing primary production with a large spatial coverage and over a broad range of temporal scales (Sathyendranath et al. 1995; Uitz et al. 2010; Chavez et al. 2011). Yet, most of these models suffer from several sources of uncertainties that generate potential errors in the production estimates (e.g. Sarmiento et al. 2004; Saba et al. 2010; Saba et al. 2011). Sources of uncertainties include, in particular, the extrapolation of the satellite chlorophyll product, which is weighted to the upper portion of the euphotic zone, to the entirety of the productive region of the water column not sensed remotely. In addition, the *in situ*-based parameterization of phytoplankton photophysiology tends to lack robustness when applied to large (regional or global) scales and over seasonal to interannual time scales.

Diel cycles observed in bio-optical properties provide a less-empirical and more mechanistic approach to assess biological production. In a seminal paper published in 1989, Siegel et al. observed the *in situ* diurnal variability of the particulate beam attenuation coefficient (c_p) and used it as a surrogate for the diurnal variations in the abundance of biogenic particles and associated production in the oligotrophic North Pacific Ocean. Several studies subsequently pursued the investigation of the diurnal variability of marine bio-optical properties as a means for determining non-intrusively *in situ* biological production (e.g. Stramska & Dickey 1992; Durand and Olson 1996; Claustre et al. 1999; Claustre 2008; Gernez et al. 2011; White et al. 2017; Briggs et al. 2018).

Among this large body of literature, Claustre et al. (2008) carried further the principle of the Siegel et al. (1989) approach for application to the South Pacific Subtropical Ocean. Based upon the generally observed relationship between the c_p coefficient and the stock of particulate organic carbon, POC (e.g. Stramski et al. 1999; Garner et al. 2006), Claustre et al.

https://doi.org/10.5194/bg-2021-123
Preprint. Discussion started: 18 May 2021

(2008) assumed that diel variations in c_p reflect diel variations in POC. Thus, the observed daytime increase and nighttime decrease in c_p-derived POC are used to estimate gross community production, community losses and, assuming equivalent day and night losses, net community production (NCP). Because the c_p coefficient is not specific to phytoplankton but includes the POC contribution of both autotrophic and heterotrophic particles, the c_p-based method yields estimate of community production.

Two studies (Kheireddine & Antoine 2014; Barnes & Antoine 2014) also attempted to extend this approach to the particulate backscattering coefficient (b_{bp}). The application opens up opportunities for assessing community production from geostationary ocean color satellite observations, from which a nearly continuous daytime b_{bp} coefficient can be retrieved. Both studies focused on surface data obtained from moored observations from the Ligurian Sea (Northwestern Mediterranean) and found weak results for the diel b_{bp} cycle, calling for further investigations.

The optics-based approach has proven to be particularly relevant for appraising particulate biological production in stratified oligotrophic systems such as subtropical gyres (e.g. Siegel et al. 1998; Claustre et al. 2008; White et al. 2017). Interestingly, in such systems, the biological production of organic carbon is difficult to quantify and potentially underestimated by ^{14}C incubation methods (Juranek & Quay 2005; Quay et al. 2010). This might be attributed to an inadequacy of traditional measurement methods for apprehending the spatial and temporal heterogeneity of biological production that may exhibit local or episodic events (Karl et al. 2003; Williams et al. 2004; McGillicuddy 2016). Moreover, in stratified oligotrophic systems, the vertical distribution of phytoplankton is frequently characterized by the presence of a deep chlorophyll maximum (DCM), also referred as subsurface chlorophyll maximum (SCM; e.g. Cullen 1982; Hense & Beckmann 2008; Cullen 2014; Mignot et al., 2014). SCMs are not necessarily resolved by *in situ* discrete sampling and

https://doi.org/10.5194/bg-2021-123
Preprint. Discussion started: 18 May 2021

cannot be observed from ocean color satellites that are limited to the surface ocean. They are typically attributed to the photoacclimation of phytoplankton cells to low light conditions (Kiefer et al. 1976; Cullen 1982; Fennel & Boss 2003; Letelier et al., 2004; Dubinsky & Stambler 2009). Yet, SCMs resulting from an actual increase in phytoplankton (carbon) biomass, and so referred to as subsurface biomass maximum (SBM), have also been observed episodically and/or seasonally in oligotrophic regions of the global ocean (Beckmann & Hense 2007; Mignot et al. 2014; Barbieux et al. 2019; Cornec et al. 2021). Considering the large (45%) surface areas covered by stratified oligotrophic regions in the global ocean (McClain et al. 2004), improving the quantification of biological production of organic carbon and characterizing the contribution of SCMs to the water-column production in such regions are critical. For this purpose, *in situ* diel-resolved measurements with high spatio-temporal resolution in the entire water column represent an intriguing opportunity.

In this study, we exploit summertime observations acquired by two BioGeoChemical-Argo (BGC-Argo) profiling floats deployed in contrasted systems of the Mediterranean Sea. This offers a unique opportunity for pursuing the exploration of the bio-optical diel cycle-based approach to biological production in oligotrophic environments. One of the two BGC-Argo floats was deployed in the Ligurian Sea in the vicinity of the BOUSSOLE fixed mooring (BOUée pour l'acquiSition d'une Série Optique à Long termE; Antoine et al. 2008). This area is representative of a seasonally stratified oligotrophic system, with a potentially productive SCM (e.g. Mignot et al. 2014; Barbieux et al. 2019) that follows a recurrent spring bloom. The second float was deployed in the Ionian Sea (Central Mediterranean) as part of the PEACETIME (ProcEss studies at the Air-sEa Interface after dust deposition in the MEditerranean sea) project (Guieu et al. 2020). The Ionian Sea is a nearly permanent oligotrophic system (e.g. Lavigne et al. 2015) with an SCM induced mostly by photoacclimation (e.g. Mignot et al. 2014; Barbieux et al. 2019).

https://doi.org/10.5194/bg-2021-123
Preprint. Discussion started: 18 May 2021

The BGC-Argo profiling floats used in this study measured, among a suite of physical and biogeochemical properties, the c_p and b_{bp} coefficients and were both programmed to sample the entire water column at a high temporal resolution (4 vertical profiles per 24h), in order to monitor the diel variations of the bio-optical properties. We applied, for the first time, a modified version of the method of Claustre et al. (2008) to the diel c_p and b_{bp} measurements acquired by the BGC-Argo floats to derive community production. Using this dataset, we (1) assess the relevance of the diel cycle-based method for estimating biological production of organic carbon in the considered regions and discuss the applicability of the method to b_{bp}, in addition to c_p; (2) investigate the regional and vertical variability of the production estimates with a focus on the SCM layer in relation to the biological and abiotic context; (3) discuss the relative contribution of the SCM layer to the water-column community production.

2 Data and methods

2.1 Study region

The Mediterranean Sea provides a unique environment for investigating the biogeochemical functioning of oligotrophic systems that exhibit either a seasonal or permanent SCM. The Mediterranean is a deep ocean basin characterized by a West-to-East gradient in nutrients and chlorophyll *a* concentration (e.g. Dugdale & Wilkerson 1988; Bethoux et al. 1992; Antoine et al. 1995; Bosc et al. 2004; D'Ortenzio & D'Alcalà 2009) associated with a deepening of the SCM (Lavigne et al. 2012; Barbieux et al. 2019). The Ionian Sea in the eastern Mediterranean is defined as permanently oligotrophic, with the SCM settled at depth over the whole year. This system represents the oligotrophic end-member type of SCM (Barbieux et al. 2019), much like the subtropical South Pacific Ocean Gyre. By contrast, the Ligurian Sea in the western Mediterranean is seasonally productive as akin to a temperate system (e.g. Casotti et al. 2003; Marty & Chiavérini 2010; Siokou-Frangou et al.

https://doi.org/10.5194/bg-2021-123
Preprint. Discussion started: 18 May 2021

2010; Lavigne et al. 2015). The mixed layer deepens significantly during the winter period, inducing seasonal renewal of nutrients in the surface layer that supports the spring bloom (Marty et al. 2002; Lavigne et al. 2013; Pasqueron de Fommervault et al. 2015; Mayot et al. 2016). After the seasonal bloom, the SBM intensifies throughout the summer and into early fall. This system represents the temperate end-member type of SCM.

We deployed BGC-Argo floats programmed for "multi-profile" sampling in each of these two regions (Fig. 1). The Ligurian Sea float (hereafter noted fLig, WMO: 6901776), was deployed in the vicinity of the BOUSSOLE fixed mooring (7°54'E, 43°22'N) during one of the monthly cruises of the BOUSSOLE program (Antoine et al. 2008). We used the fLig float measurements acquired during the time period May 24 to September 13, 2014. The Ionian Sea float (hereafter noted fIon, WMO: 6902828) was deployed as part of the PEACETIME project (Guieu et al. 2020). We used the fIon float measurements acquired during the time period May 28 to September 11, 2017. Thus, although collected in different years, the data sets arise from similar seasonal contexts.

2.2 BGC-Argo multi-profiling floats and data processing

The BGC-Argo floats used in this study are "PROVOR CTS-4" (nke Instrumentation, Inc.). They were both equipped with the following sensors and derived data products: (1) a CTD sensor for depth, temperature and salinity; (2) a "remA" combo sensor that couples a SAtlantic OCR-504 (for downwelling irradiance at three wavelengths in addition to photosynthetic available radiation, PAR) and a WET Labs ECO Puck Triplet (for both chlorophyll *a* (excitation/emission wavelengths of 470 nm/695 nm) and colored dissolved organic matter (CDOM; 370 nm/460 nm) fluorescence, and particulate backscattering coefficient at 700 nm); and (3) a WET Labs C-Rover (for particulate beam attenuation coefficient at 660 nm, 25-cm pathlength). Data were collected along water column profiles from 1000 m up to the surface with a vertical resolution of 10 m between 1000 and 250 m, 1

https://doi.org/10.5194/bg-2021-123
Preprint. Discussion started: 18 May 2021

187 m between 250 and 10 m, and 0.2 m between 10 m and the surface. First, the BGC-Argo raw
188 counts were converted into geophysical units by applying factory calibration. Second, we
189 applied corrections following the BGC-Argo QC procedures (Schmechtig et al. 2015, 2016;
190 Organelli et al. 2017).

191 Factory-calibrated chlorophyll fluorescence requires additional corrections for
192 determining the chlorophyll *a* concentration (Chl). Values collected during daylight hours
193 were corrected for non-photochemical quenching following Xing et al. (2012). A global
194 analysis of factory-calibrated chlorophyll fluorescence measured with WET Labs ECO
195 sensors relative to concurrent chlorophyll *a* concentrations, determined by High Performance
196 Liquid Chromatography (HPLC), yielded a global overestimate bias of 2 (Roesler et al. 2017),
197 with statistically significant regional biases varying between 0.5 and 6. In the Mediterranean
198 Sea, the regional variations of the fluorescence-to-Chl ratio are known to be very small
199 (Taillandier et al. 2018), hence the bias correction factor of 2 was applied to BGC-Argo
200 fluorescence data from both the Ligurian and Ionian regions, consistently with the processing
201 performed at the Coriolis Data Center.

202 For the particulate backscattering coefficient (b_{bp}), we followed the BGC-Argo
203 calibration and quality control procedure of Schmechtig et al. (2016). The backscattering
204 coefficient at 700 nm (m^{-1}) is retrieved following Eq. (1):

205 $$b_{bp}(700) = 2\,\pi\,\chi\,[(\beta b_{bp} - Dark b_{bp}) \times Scale b_{bp} - \beta sw] \quad (1)$$

206 where $\chi = 1.076$ is the empirical weighting function that converts particulate volume
207 scattering function at 124° to total backscattering coefficient (Sullivan et al. 2013); βb_{bp} is
208 the raw observations from the backscattering meter (digital counts); $Dark b_{bp}$ (digital counts)
209 and $Scale b_{bp}$ (m^{-1} sr^{-1} $count^{-1}$) are the calibration coefficients provided by the manufacturer;
210 and βsw is the contribution to the Volume Scattering Function (VSF) by the pure seawater at

https://doi.org/10.5194/bg-2021-123
Preprint. Discussion started: 18 May 2021

211 the 700 nm measurement wavelength that is a function of temperature and salinity (Zhang et
212 al. 2009).

213 The calibration procedure applied to the particulate beam attenuation coefficient (c_p) is
214 similar to that described in Mignot et al. (2014). The beam transmission, T (%), is
215 transformed into the beam attenuation coefficient, c (m^{-1}), using the relationship:

216 $$c = -\frac{1}{x} \ln \frac{T}{100} \quad (2)$$

217 where x is the transmissometer pathlength (25 cm). The beam attenuation coefficient c is the
218 sum of the absorption and scattering by seawater and its particulate and dissolved
219 constituents. At 660 nm, the contribution of CDOM (c_{cdom}) can be considered negligible in
220 oligotrophic waters because, although its absorption in the blue is comparable to that of
221 particulate material (Organelli et al. 2014), the c_{cdom} spectrum decays exponentially towards
222 near zero in the red (Bricaud et al. 1981), and because it is comprised of dissolved molecules
223 and colloids, its scattering is negligible (Boss and Zaneveld 2003). Meanwhile $c_w(660)$ for
224 pure water is constant and removed in the application of the factory calibration; effects due to
225 dissolved salt are accounted for according to Zhang et al. (2009). Hence, at a wavelength of
226 660 nm, the particle beam attenuation coefficient, c_p (m^{-1}), is retrieved by subtracting the
227 seawater contribution to c. The biofouling-induced increasing signal observed in clear deep
228 waters and resulting in a drift in c_p values with time, is corrected as follows. For each profile,
229 a median c_p value, used as an "offset", is computed from the c_p values acquired between 300
230 m and the maximum sampled depth, and subtracted from the entire profile.

231 Using the solar noon Photosynthetically Available Radiation (PAR) measurements, we
232 computed the euphotic layer depth (Z_{eu}) as the depth at which the PAR is reduced to 1% of its
233 value just below the surface (Gordon & McCluney 1975) and the penetration depth (Z_{pd}; also
234 known as the e-folding depth or first attenuation depth) as Z_{eu} / 4.6. We define the surface

https://doi.org/10.5194/bg-2021-123
Preprint. Discussion started: 18 May 2021

235 layer from 0 m to Z_{pd}. We also define the SCM layer as in Barbieux et al. (2019), whereby a
236 Gaussian model is fit to each Chl vertical profile in order to determine the depth interval of
237 the full width half maximum of the SCM. Finally, the Mixed Layer Depth (MLD) is derived
238 from the float CTD data as the depth at which the potential density difference relative to the
239 surface reference value is 0.03 kg m^{-3} (de Boyer Montégut et al. 2004).

240 Unlike the majority of BGC-Argo floats that collect profile measurements every 10
241 days, the two platforms used in this study sampled the water column 4 profiles per day, albeit
242 with slightly different regimes (Fig. 2). The fLig float cycle commences with the first profile
243 at solar noon (t_n), a second at sunset the same day (t_{ss}), a third profile at sunrise the next day
244 (t_{sr+1}), and a last one at solar noon the next day (t_{n+1}). The sampling cycle is repeated every
245 four days. The fIon cycle is performed over a single 24-hour period; it begins at sunrise (t_{sr}),
246 followed by a second profile at solar noon (t_n), a third at sunset (t_{ss}) and a last night profile at
247 approximately midnight (t_m). For this float, the sampling cycle is repeated each day.

248 **2.3 Characterization of the diel cycle of the bio-optical properties**

249 In order to characterize the amplitude and variability of the diel cycle of the c_p and b_{bp}
250 coefficients, we use the metrics defined by Kheireddine & Antoine (2014). We compute the
251 relative daily variation $\tilde{\Delta}c_p$ and $\tilde{\Delta}b_{bp}$ (expressed as % change) for each float and each day of
252 observation, from sunrise to sunrise (fIon) as follows:

253 $$\tilde{\Delta}c_p = 100\left(\frac{c_p(t_{sr})}{c_p(t_{sr+1})} - 1\right) \quad (3)$$

254 $$\tilde{\Delta}b_{bp} = 100\left(\frac{b_{bp}(t_{sr})}{b_{bp}(t_{sr+1})} - 1\right) \quad (4)$$

255 with $c_p(t_{sr})$ and $b_{bp}(t_{sr})$ being the values of c_p and b_{bp} at sunrise and $c_p(t_{sr+1})$ and
256 $b_{bp}(t_{sr+1})$ the values at sunrise the next day. Comparable computations for fLig were made

https://doi.org/10.5194/bg-2021-123
Preprint. Discussion started: 18 May 2021

from noon (t_n) to noon (t_{n+1}). Then the mean and range in relative daily variations ($\widetilde{m\Delta}$ and $\widetilde{r\Delta}$, respectively) are computed for each float over the entire time series.

2.4 Principle of the bio-optical diel cycle-based approach to biological production

In this study we considered two distinct bio-optical properties, i.e. the c_p coefficient (Siegel et al. 1989; Claustre et al. 2008) and the b_{bp} coefficient (Barnes & Antoine 2014; Kheireddine & Antoine 2014). To first order, c_p and b_{bp} are linearly correlated to, and thus may be used as a proxy for, the stock of POC (e.g. Oubelkheir et al. 2005; Gardner et al. 2006; Cetinić et al. 2012). Both of these bio-optical proxies have been shown to exhibit a diurnal cycle (e.g. Oubelkheir & Sciandra 2008; Loisel e al. 2011; Kheireddine & Antoine 2014).

The daily solar cycle is a major driver of biological activity in all oceanic euphotic zones (e.g. Oubelkheir & Sciandra 2008), which influences the abundance of microorganisms (Jacquet et al. 1998; Vaulot & Marie 1999; Brunet et al. 2007) and therefore, the magnitude of the c_p and b_{bp} coefficients. To first order, the diurnal increase in c_p or b_{bp} may be attributed to an increase in particle biomass, resulting from an increase in particle abundance and/or size, both associated with cell division. To second order, the diurnal increase in c_p or b_{bp} may be caused by variations in particle shape and refractive index (Stramski & Reynolds 1993; Durand & Olson 1996; Claustre et al. 2002; Durand et al. 2002). The night decrease in c_p or b_{bp} may be explained by a decrease in particle abundance due to particle aggregation and sinking or grazing (Cullen et al. 1992), changes in particle size and/or refractive index associated with cell division, or microorganism respiration.

The bio-optical diel cycle-based approach used in this study relies on a modified version of Claustre et al. (2008). Following this approach, the observed daytime increase and nighttime decrease in c_p-derived (or b_{bp}-derived) POC are used to estimate gross community

https://doi.org/10.5194/bg-2021-123
Preprint. Discussion started: 18 May 2021

production. For this purpose, the c_p and b_{bp} coefficients, measured *in situ* by the BGC-Argo profiling floats, are converted into POC equivalent using a constant c_p-to-POC (or b_{bp}-to-POC) relationship from the literature (see below). By definition, the c_p and b_{bp} coefficients target particles so that the dissolved biological matter is not accounted for by the present method.

2.5 Bio-optical properties-to-POC relationships

The conversion of c_p and b_{bp} into POC relies on the use of empirical proxy relationships and assumptions concerning the variations in those relationships. First, as in Claustre et al. (2008), we assume that the c_p- or b_{bp}-to-POC relationship remains constant on a daily timescale, consistently with previous works (Stramski & Reynolds 1993; Cullen & Lewis 1995), so that observed variations in the optical coefficients can be interpreted as variations in POC. Second, the specific proxy value is not constant, as many empirical relationships between POC and c_p (e.g. Claustre et al. 1999; Oubelkheir et al. 2005; Gardner et al. 2006; Loisel et al. 2011) or b_{bp} (e.g. Stramski et al. 2008; Loisel et al. 2011; Cetinić et al. 2012) have been proposed for specific regions (Tables 1 and 2). In the present study, we used the relationships from Oubelkheir et al. (2005) and Loisel et al. (2011) for c_p and b_{bp}, respectively. Both relationships were established from *in situ* measurements collected in the Mediterranean Sea and produce c_p- or b_{bp}-derived POC values falling in the middle of the range of all the POC values resulting from the different bio-optical relationships taken from the literature (Tables 1 and 2).

2.6 Estimating biological production from the diel cycle of POC

2.6.1 Hypotheses

The time-rate-of-change in depth-resolved POC biomass, b(z,t), can be described by a partial differential equation:

https://doi.org/10.5194/bg-2021-123
Preprint. Discussion started: 18 May 2021

$$\frac{\partial b(z,t)}{\partial t} = \mu(z,t)\, b(z,t) - l(z,t)\, b(z,t), \quad (5)$$

where $\mu(z,t)$ is the particle photosynthetic growth rate and $l(z,t)$ the particle loss rate at depth z and time t (both in units of d^{-1}). As in previous studies (Claustre et al. 2008, Gernez et al. 2011; Barnes and Antoine 2014), we assume a quasi-1D framework. In other words, we ignore the effects of lateral transport of particles by oceanic currents and assume that there is no vertical transport of particles in and out the layer considered. We also assume that the loss rate is constant throughout the day and uniform with depth, i.e. $l(z,t) = l$. In this context, the time series of profiles are first converted to depth-integrated biomass (from b(z,t) to B(t)) for each of the layers in question, and then integrated over time to determine daytime gain, nighttime loss, and net daily production.

2.6.2 Calculation of the loss rate

During nighttime, there is no photosynthetic growth, so that Eq. (5) becomes:

$$\frac{\partial b(z,t)}{\partial t} = l\, b(z,t). \quad (6)$$

The integration of Eq. (6) over depth yields an expression of the rate of change of the depth-integrated POC biomass, $B(t)$:

$$\frac{\partial B(t)}{\partial t} = -\, l\, B(t), \quad (7)$$

with $B(t) = \int_{z2}^{z1} b(z,t)dz$, the POC integrated within a given layer of the water column, comprised between the depths z_1 and z_2 (in gC m^{-2}). In this respect, we consider three different layers: the euphotic layer extending from z_1 = 0 m to z2 = Z_{eu}; the surface layer extending from z_1 = 0 m to z2 = Z_{pd}; and the SCM layer extending from z1 = Z_{SCM} - $Z_{SCM,1/2}$ and z2 = Z_{SCM} + $Z_{SCM,1/2}$, with Z_{SCM} the depth of the SCM and $Z_{SCM,1/2}$ the depth at which Chl is half of the SCM value.

https://doi.org/10.5194/bg-2021-123
Preprint. Discussion started: 18 May 2021

Eq. (7) can be integrated over nighttime to obtain an equation for the loss rate *l*, as a function of the nocturnal variation of B:

$$l = \frac{\ln\left(\frac{B_{ss}}{B_{sr+1}}\right)}{t_{sr+1} - t_{ss}}, \quad (8)$$

with $B(t_{ss})$ and $B(t_{sr+1})$ corresponding to the POC integrated within the layer of interest, at t_{ss} (sunset) and t_{sr+1} (sunrise of the next day).

2.6.3 Calculation of the production rate

The daily and depth-integrated production of particles, P (in units of gC m^{-2} d^{-1}), is defined as:

$$P = \int_{t_{sr}}^{t_{sr+1}} \int_{z2}^{z1} \mu(z,t)\, b(z,t)\, dz\, dt, \quad (9)$$

with t_{sr} the time of sunrise on day 1 and t_{sr+1} the time of sunrise the following day. Equation (5) can be used to express P as a function of *l*, b(z,t), and the rate of change of b(z,t):

$$P = \int_{t_{sr}}^{t_{sr+1}} \int_{z2}^{z1} \left(\frac{\partial b(z,t)}{\partial t} + l\, b(z,t)\right) dz\, dt, \quad (10)$$

which yields:

$$P = B_{t_{sr+1}} - B_{t_{sr}} + l \int_{t_{sr}}^{t_{sr+1}} B(t)\, dt. \quad (11)$$

Finally, using the trapezoidal rule, Eq. (11) simplifies into

$$P = B_{t_{sr+1}} - B_{t_{sr}} + l \sum_{i=1}^{j} (t_{i+1} - t_i) \frac{B_{i+1} + B_i}{2}, \quad (12)$$

with *l* calculated from Eq. (8) and the index i corresponding to the different measurement time steps over the course of the diel cycle (t_n, t_{ss}, t_{sr+1}, and t_{n+1} for the Ligurian Sea, and t_{sr}, t_n, t_{ss}, and t_m for the Ionian Sea; Fig. 2).

In brief, Eq. (12) is applied to the time series of the BGC-Argo floats by using b_{bp} and c_p converted into POC equivalents, integrated within the euphotic, surface, and SCM layers to

https://doi.org/10.5194/bg-2021-123
Preprint. Discussion started: 18 May 2021

348 compute c_p- and b_{bp}-derived estimates of gross community production, P, in all three layers of
349 the water column.

350 **2.7 Primary production model**

351 The community production estimates obtained from the bio-optical diel cycle-based
352 method are evaluated against primary production values computed with the bio-optical
353 primary production model of Morel (1991). Morel's model estimates the daily depth-resolved
354 organic carbon concentration fixed by photosynthesis, using the noontime measurements of
355 Chl, temperature and PAR within the water column by the BGC-Argo profiling floats as
356 model inputs. The standard phytoplankton photophysiological parameterization is used for
357 these calculations (Morel 1991; Morel et al. 1996).

358 **2.8 Phytoplankton pigments and community composition**

359 During the BOUSSOLE cruises conducted in 2014 (cruises #143 to #154) and the
360 PEACETIME cruise, discrete seawater samples were taken at 10–12 depths within the water
361 column from Niskin bottles mounted on a CTD-rosette system and then filtered under low
362 vacuum onto Whatman GF/F filters (0.7-µm nominal pore size, 25-mm diameter). The filters
363 were flash-frozen in liquid nitrogen and stored at -80°C until analysis by HPLC following the
364 protocol of Ras et al. (2008). The concentrations of phytoplankton pigments resulting from
365 these analyses were used to estimate the composition of the phytoplankton assemblage. For
366 this purpose, we used the diagnostic pigment-based approach (Claustre et al. 1994; Vidussi et
367 al. 2001; Uitz et al. 2006) with the coefficients of Di Cicco et al. (2017) to account for the
368 specificities of Mediterranean phytoplankton communities. This approach yields the relative
369 contribution to chlorophyll *a* biomass of major taxonomic groups merged into three size
370 classes (micro-, nano and picophytoplankton).

https://doi.org/10.5194/bg-2021-123
Preprint. Discussion started: 18 May 2021

371 The fLig float was spatially distanced from the location of sampling at the BOUSSOLE
372 mooring site. Thus it was necessary to identify the time shift for matching the cruise-sampled
373 analyses to the float profile measurements. This was achieved by performing a cross-
374 correlation analysis of the bio-optical time series measurements collected on the float with
375 that on the mooring (in this case Chl, c_p and b_{bp}). A positive time lag between the
376 BOUSSOLE site and the position of the fLig float during its drift is observed suggesting that
377 the variations observed by the float led that observed at BOUSSOLE by ~2 days. This small-
378 time lag coupled with high correlation coefficient values and long decorrelation time scales,
379 indicate that the monthly interpolated pigment data measured at the BOUSSOLE site may be
380 considered as representative of the pigment composition along the fLig float trajectory.

381 ## 3 Results and discussion

382 In this section, we first provide an overview of the biogeochemical and bio-optical
383 characteristics measured by the two BGC-Argo profiling floats in the Ligurian and Ionian
384 Seas. We then assess the usefulness of the diel cycle of the b_{bp} coefficient for deriving
385 community production, in comparison to the c_p-derived estimates as a reference, and discuss
386 the c_p-derived estimates. Finally, we examine the community production estimates in both
387 study regions, with an emphasis on the SCM layer and its biogeochemical significance.

388 ### 3.1 Biogeochemical and bio-optical context in the study regions

389 Both study regions are characterized by either seasonal or persistent oligotrophy, with
390 mean surface Chl values ranging within 0.08–0.22 mg m^{-3} (Fig. 3), and a stratified water
391 column with a consistently shallow MLD (<30 m). They do exhibit very different euphotic
392 zones, with a mean Z_{eu} of 47±5 m and 89±4 m in the Ligurian and Ionian Seas, respectively.
393 Both regions also display a SCM, the depth of which co-occurs with Z_{eu} and the isopycnal
394 28.85 (i.e. the isoline of potential density 28.85 kg m^{-3}) over the considered time series,

https://doi.org/10.5194/bg-2021-123
Preprint. Discussion started: 18 May 2021

except for the last month of observation in the Ionian Sea. In the Ligurian Sea, the SCM is intense (1.06±0.34 mg Chl m^{-3}; Fig. 3a), relatively shallow (41±7 m), and associated with the subsurface c_p and b_{bp} maxima (0.27±0.09 and 0.0015±0.0006 m^{-1}, respectively; Fig. 3b–c). The Chl, and c_p values are 5 times larger in the SCM layer than at surface, and the b_{bp} values 3.6 times larger. In contrast, in the Ionian Sea, the SCM is associated with lower values of Chl (0.27±0.07 mg m^{-3}; Fig. 3d), c_p (0.05±0.01 m^{-1}; Fig. 3e) and b_{bp} (0.0005±0.0001 m^{-1}; Fig. 3f). Compared to the Ligurian Sea SCM, the Ionian Sea SCM is located twice as deep (97±11 m) and is uncoupled from any c_p and b_{bp} maxima that occur at shallower depth. Hence, the selected regions are representative of two contrasted SCM systems with distinct degree of oligotrophy, consistent with our expectations (e.g. D'Ortenzio & Ribera D'Alcalà 2009; Barbieux et al. 2019). These observations indeed suggest that the Ligurian Sea SCM mirrors an increase in phytoplankton carbon biomass (SBM) likely resulting from favorable light and nutrient conditions, whereas the Ionian SCM is induced by photoacclimation of phytoplankton cells.

Although the summer period is typically considered stable, some temporal variations are observed over the time series that are more pronounced in the SCM layer than at surface. In the Ligurian Sea SCM, the Chl, c_p and b_{bp} exhibit similar temporal evolution, with relatively high values in late May 2014, followed by a marked decrease until mid-July (Figs. 4a–c). Then we observe two minima in Chl, c_p and b_{bp} that delineate a second peak between July 14 and August 16, 2014 (as indicated by the dashed lines in Fig. 4a–c). In the Ionian Sea SCM, the Chl, c_p and b_{bp} values all decrease from late May until a minimum is reached on August 11, 2017 (dashed line in Figs. 4d–e) and a second increase is recorded later in the season. These temporal patterns are further discussed (Section 3.4).

https://doi.org/10.5194/bg-2021-123
Preprint. Discussion started: 18 May 2021

418 **3.2 Assessment of the method**

419 **3.2.1 Analysis of the diel cycle of the b_{bp} coefficient**

420 Diel cycles, characterized by a daytime increase and a nighttime decrease, are observed in
421 both c_p and b_{bp} time series in all three layers of the water column (Fig. 5). In the surface layer
422 of the Ligurian Sea, the diel cycles of c_p and b_{bp} exhibit, respectively, mean relative daily
423 variation ($\widetilde{m\Delta}$) of 12.7% and 2.3%, and a range in relative daily variations ($\widetilde{r\Delta}$) of 256.7% and
424 28.5% (Table 3). These values are of the same order of magnitude as those reported by
425 Kheireddine & Antoine (2014), acquired from the BOUSSOLE surface mooring in the same
426 area and during the oligotrophic season (from -5% to 25% for c_p and from -2% to 10% for
427 b_{bp}). Interestingly, the diel cycle of the c_p coefficient appears systematically more pronounced
428 than that of b_{bp}, with larger values of $\widetilde{m\Delta}$ and $\widetilde{r\Delta}$, regardless of the considered region and layer
429 of the water column (Table 3).

430 To first order, the variability in the b_{bp} and c_p coefficients is determined by the variability
431 in particle concentration, which underpins their robustness as POC proxies in open-ocean
432 conditions and explains their coherent evolution on a monthly timescale (Figs. 3–4).
433 Nevertheless, to second order, these coefficients vary differentially with the size and
434 composition of the particle pool. In particular, phytoplankton make a larger contribution to c_p
435 than b_{bp}, in part due to their strong absorption efficient. In addition, b_{bp} is more sensitive to
436 smaller (<1 µm) particles (Stramski & Kiefer 1991; Ahn et al. 1992; Stramski et al. 2001;
437 Boss et al. 2004) and to particle shape and internal structure (Bernard et al. 2009;
438 Neukermans et al. 2012; Moutier et al. 2017; Organelli et al. 2018) than is c_p. While the diel
439 cycle of c_p would be essentially driven by photosynthetic processes due to the influence of
440 phytoplankton on c_p, b_{bp} would be more responsive to detritus and/or heterotrophic bacteria
441 that show minor, if not negligible, daily variability. Hence, such specificities in the bio-optical
442 coefficients may explain the observed differences in their diel cycles.

https://doi.org/10.5194/bg-2021-123
Preprint. Discussion started: 18 May 2021

Based on high-frequency surface measurements in the Ligurian Sea in various seasons, the studies of Kheireddine & Antoine (2014) and Barnes & Antoine (2014) demonstrated that the diel cycle of b_{bp} not only exhibits much reduced relative amplitude compared to that of c_p, but the features of the b_{bp} cycle are not synchronous with that of the c_p cycle. Thus b_{bp} cannot be used interchangeably with c_p for assessing daily changes in POC or community production. Our results support these previous findings, not only for the surface layer of the Ligurian Sea, but also for the whole water column of both the Ligurian and Ionian regions.

We now consider the integrated euphotic zone gross community production estimates derived from the bio-optical diel cycle-based method (Fig. 6). We compare the c_p- and b_{bp}-based estimates with primary production estimates computed with the model of Morel (1991). The b_{bp}-derived production rates underestimate those derived from c_p in both regions by about a factor of ten, with respective mean values of 0.11±0.28 gC m^{-2} d^{-1} and 1.18 ±1.13 gC m^{-2} d^{-1} in the Ligurian Sea, and 0.04±0.04 gC m^{-2} d^{-1} and 0.46 ±0.11 gC m^{-2} d^{-1} in the Ionian Sea. In addition, the b_{bp}-derived production is much lower than the primary production computed with the model of Morel (1991), which has mean values of 0.91±0.14 gC m^{-2} d^{-1} in the Ligurian Sea and 0.31 ±0.04 gC m^{-2} d^{-1} in the Ionian Sea. The significantly lower community production rates are a direct effect of the dampened relative daily amplitude of the b_{bp} diel cycle (Table 3), and the sensitivity of b_{bp} to the smaller heterotrophic and detrital particulate matter. These bio-optical diel cycle-based method, whether applied to c_p or b_{bp}, yields an estimate of the community production, i.e. that associated with the accumulation of phytoplankton *and* bacteria biomass, which is necessarily larger than the primary (photo-autotrophic) production rates from the Morel (1991) model. These questionable low values of community production, along with the observation of a weak daily variability in b_{bp}, support the idea that the diel cycle of b_{bp} may not be a reliable index for total community production rates, consistently with previous studies (Kheireddine & Antoine 2014; Barnes & Antoine

https://doi.org/10.5194/bg-2021-123
Preprint. Discussion started: 18 May 2021

468 2014). However, the utility of a b_{bp}-derived community production may be revealed in
469 elucidating rates for distinct size-based groups of organisms, such as picoplankton. A better
470 understanding of the specific size range that dominates the diel cycle in b_{bp} will be important
471 to understand. Yet, for our purposes, we disregard the b_{bp}-based estimates and focus our
472 analysis on the c_p-derived gross community production estimates.

473 **3.2.2 Community production derived from the c_p coefficient**

474 The c_p-derived estimates of gross community production, integrated within the euphotic
475 layer, compare favorably with those found in the literature for similar Mediterranean areas
476 (see Table 4 and references therein). The c_p-based estimates show a 2.5-fold difference
477 between the Ligurian Sea and the Ionian Sea (mean of 1.18 gC m^{-2} d^{-1} and 0.46 gC m^{-2} d^{-1},
478 respectively; Table 6). In comparison, water column-integrated primary production values,
479 either inferred from satellite observations and biogeochemical models or measured *in situ*,
480 vary within the range 0.13–1 gC m^{-2} d^{-1} and 0.14–0.69 gC m^{-2} d^{-1} for the Western (or
481 Ligurian) and Eastern (or Ionian) region, respectively (Table 4). As expected, our c_p-based
482 community production rates are larger than published primary production rates. The present
483 c_p-derived values also compare favorably with gross community production estimates inferred
484 from a similar approach applied to bio-optical measurements from the BOUSSOLE mooring
485 in the Ligurian Sea (0.8–1.5 gC m^{-2} d^{-1} in May–August; Barnes & Antoine 2014) and along an
486 oligotrophic gradient in the South Pacific Subtropical Ocean (0.85 gC m^{-2} d^{-1}; Claustre et al.
487 2008).

488 The empirical relationships linking the c_p (or b_{bp}) coefficient to POC are known to exhibit
489 regional and seasonal variability in response to changes in the composition of the particle
490 assemblage and associated changes in particle size, shape and type, i.e. biogenic or mineral
491 (e.g. Stramski et al. 2004; Neukermans et al. 2012; Slade & Boss 2015). Hence, the choice of
492 such relationships strongly affects the conversion of the measured daily bio-optical variability

https://doi.org/10.5194/bg-2021-123
Preprint. Discussion started: 18 May 2021

493 into POC fluxes. For the time period and study regions here, the c_p-based community
494 production varies by a factor of 2, depending on the selected bio-optical relationship, so that
495 c_p-based estimates vary between 0.89±0.84 gC m^{-2} d^{-1} and 1.62±1.54 gC m^{-2} d^{-1} in the
496 Ligurian Sea, and between 0.35±0.09 gC m^{-2} d^{-1} and 0.63±0.16 gC m^{-2} d^{-1} in the Ionian Sea.
497 The minimal and maximal values are obtained with the bio-optical relationships from Marra
498 et al. (1995) and Stramski et al. (2008), respectively (Table 5). Compared to the reference
499 value obtained using the Oubelkheir et al. (2005) relationship, the c_p-based estimates are 25%
500 lower and 37% higher using the relationships of Marra et al. (1995) and Stramski et al.
501 (2008), respectively.

502 The use of the single relationship established from Mediterranean waters (Oubelkheir et
503 al. 2005) appears as a reasonable choice for the study region. Yet, if more relevant bio-optical
504 proxy relationships are available, such as one that accounts for spatial and seasonal variations,
505 and even applicable to different layers of the water column, that would certainly reduce the
506 uncertainty in the rate estimation. Although this is beyond the scope of the present study, we
507 recognize that such investigations should be conducted in the future in order to refine optics-
508 based biomass (POC) and community production estimates.

509 **3.3 Regional and vertical variability of production**

510 The temporal evolution of the c_p-derived POC biomass integrated within the three
511 distinct layers of the water column is presented for the two study regions in Fig. 7. The
512 integrated POC concentration values follow similar temporal trends as reported for c_p (Figs.
513 3–4). In the Ligurian Sea, the euphotic layer-integrated POC varies between 1.5 and 6.0 gC
514 m^{-2} (mean of 3.7±1.1 gC m^{-2}; Fig. 7a and Table 6). There was a decrease from late May to
515 mid-July (6.0 to 1.5 gC m^{-2}) followed by a moderate peak (3.9 gC m^{-2}) between mid-July and
516 mid-August (as bounded by the dashed lines in Fig. 5). The c_p-based community production
517 did exhibit large variability over the time period (Fig. 7b and Table 6), but interestingly, the

https://doi.org/10.5194/bg-2021-123
Preprint. Discussion started: 18 May 2021

518 moderate POC peak observed in the core of the oligotrophic season (between mid-July and
519 mid-August) is associated with the maximum production rate of the time series (4.3 gC m^{-2} d^{-1}).

521 In the Ionian Sea, the POC biomass integrated within the euphotic zone is much lower
522 than in the Ligurian Sea and remains more stable over the time period (1.9±0.24 gC m^{-2}; Fig.
523 7c and Table 6). As with POC, the community production is much lower in the Ionian Sea
524 than in the Ligurian Sea, but still exhibits substantial variability with values ranging within
525 0.06–0.68 gC m^{-2} d^{-1} (Fig. 7d). These results are consistent with multiple studies reporting a
526 large difference in the trophic status and productivity of the Ligurian and Ionian Seas, on
527 seasonal and annual timescales (D'Ortenzio & Ribera d'Alcala, 2009; Siokou-Frangou et al.
528 2010; Lavigne et al. 2013; Mayot et al. 2016). Our results confirm this difference, yet on a
529 monthly timescale during the oligotrophic summer period.

530 The gross community production estimates integrated over different layers of the
531 water column reveal distinct patterns. In the Ligurian Sea, both the euphotic and SCM layers
532 show large production rates (0.96±1.3 gC m^{-2} d^{-1}), with production in the SCM layer
533 frequently equaling or overtaking on the production in the euphotic layer (Fig. 7b). This is
534 particularly striking in late July, when the production peak is actually associated with a large
535 enhancement of the production in the SCM layer (4.9 gC m^{-2} d^{-1}). In contrast, the surface
536 layer shows reduced production rates (0.29±0.33 gC m^{-2} d^{-1}), a pattern also observed in the
537 Ionian Sea (0.11±0.04 gC m^{-2} d^{-1}). In the Ionian Sea, the production is maximal in the
538 euphotic zone, and very variable and occasionally larger in the SCM layer (0.14±0.39 gC m^{-2}
539 d^{-1}; Fig. 7d). The bio-optical diel cycle-based method produces several occurrences of
540 negative values in the SCM layer, indicating that the quasi-1-D assumption is occasionally not
541 satisfied in the lower part of the euphotic layer. This could arise when physical processes that
542 transport particles are larger than local growth and loss of POC.

https://doi.org/10.5194/bg-2021-123
Preprint. Discussion started: 18 May 2021

Our results support the hypothesis raised in previous studies (e.g. Mignot et al. 2014; Barbieux et al. 2019) that, in the Ligurian temperate-like system, the SCM, which is in fact an SBM, may be highly productive. Conversely, in the Ionian region, which shows similarities with subtropical stratified oligotrophic systems, the SCM reflects photoacclimation and is less productive. Beyond these mean regional trends, both SCM systems exhibit some temporal variability in production, a somewhat unexpected pattern at the core of the presumably stable oligotrophic season.

3.4 Production in the SCM layer in relation with the biotic and abiotic context

Here we investigate the temporal variability in the SCM layer production and attempt to interpret the observed patterns in the context of biological and abiotic conditions.

3.4.1 Phytoplankton and particulate assemblage

The pigment data collected during the BOUSSOLE and PEACETIME cruises concomitantly with the deployments of the fLig and fIon floats, respectively, are used as proxies for phytoplankton community structure (Fig. 8). In the Ligurian Sea, nanophytoplankton (mainly prymnesiophytes) appear as dominant contributors to the phytoplankton assemblage both in the surface layer (48±8%; Fig. 8b) and SCM layer (54±10%). Picophytoplankton (prokaryotes and small chlorophytes) and microphytoplankton (diatoms and dinoflagellates) are present in moderate proportions, with 30±11% and 22±5% in the upper layer, and 19±7% and 27±9% in the SCM layer, respectively (Figs. 8a and 8c). No marked community change is observed during the timeseries. In the Ionian Sea, the surface layer displays large contribution of nanophytoplankton (56±2%; Fig. 8e) and, to a lesser extent, picophytoplankton (29±3%; Fig. 8d). However, the SCM level is characterized by an enhanced contribution of microphytoplankton (diatoms) to the algal assemblage (49±5%; Fig. 8f), as discussed in Marañon et al. (2021). The Ionian PEACETIME data was

https://doi.org/10.5194/bg-2021-123
Preprint. Discussion started: 18 May 2021

567 limited to the period from May 25 to 28, 2017, and thus it was not possible to determine
568 whether the composition of phytoplankton communities evolved with time. Although not
569 characterized by the prokaryotic populations (*Synechococcus* and *Prochlorococcus*) that
570 typically prevail in stratified oligotrophic environments, our observations are consistent with
571 previous studies reporting enhanced contributions of nanophytoplankton (e.g. Gitelson et al.
572 1996; Vidussi et al. 2001) and the occurrence of diatoms at depth (Siokou-Frangou et al.
573 2010; Crombet et al. 2011; Marañon et al. 2021) in the Mediterranean Sea.

574 Bio-optical properties and their ratios provide indication about variations in the
575 constituents (algal or nonalgal) and size of the particulate pool, the composition of the
576 phytoplankton assemblage and the physiological status of phytoplankton cells (e.g. Geider
577 1987; Ulloa et al. 1994; Stramski et al. 2004; Loisel et al. 2007). Here we consider the bio-
578 optical ratios b_{bp} / c_p, c_p / Chl, and b_{bp} / Chl in the SCM layer (Fig. 9). The b_{bp} / c_p ratio, while
579 at slightly different wavelengths (700 nm and 660 nm, respectively) are at absorption minima
580 and thus this ratio is comparable to the backscattering ratio b_{bp} / b_p. The b_{bp} / b_p ratio is a
581 demonstrated proxy for determining relative constituent composition (Twardowski et al.
582 2001), with phytoplankton exhibiting lower ratios than nonalgal particles (approximately
583 0.5% and 1%, respectively; Boss et al. 2004; Whitmire et al. 2007; Westberry et al. 2010).
584 The b_{bp} / Chl and c_p / Chl ratios are both proxies for the POC / Chl ratio (e.g. Claustre et al.
585 1999; Oubelkheir et al. 2005; Behrenfeld et al. 2015; Álvarez et al. 2016), and thus an
586 indicator of the contribution of phytoplankton to the whole organic pool. The variations are
587 also interpreted as changes in the composition of phytoplankton communities (e.g.
588 Sathyendranath et al. 2009) and their acclimation to the light-nutrient regime (e.g. Geider et
589 al. 1987; Geider et al. 1997; Cloern 1999) if one assumes that nonalgal particles are negligible
590 (e.g., as indicated by the backscattering ratio) or not varying in concentration. The differences
591 between the b_{bp} / Chl and c_p / Chl ratios lie in the fact that they are sensitive to different

https://doi.org/10.5194/bg-2021-123
Preprint. Discussion started: 18 May 2021

592 particle size ranges (Roesler and Boss 2008) and, thus, when they are not correlated, one can
593 qualitatively discern differing dynamics across the phytoplankton size spectrum.

594 The b_{bp} / c_p ratio is very different between the Ligurian and Ionian Seas, with significantly
595 lower values in the Ligurian Sea (0.0068±0.0009 or 0.68±0.09%, and 0.0095±0.0009 or
596 0.95±0.09%; Fig. 9). These ratios indicate that, in the general sense, the Ligurian Sea SCM is
597 more phytoplankton dominated than the Ionian Sea SCM, which tends towards nonalgal
598 particles. In the Ligurian Sea, the b_{bp} / c_p ratio remains <0.0087 (0.87%) and reaches a
599 minimum of 0.0055 (0.55%) over the period coinciding with the production event from mid-
600 July to mid-August (Fig. 9a), consistent with phytoplankton dominance. In contrast, in the
601 Ionian Sea SCM, the b_{bp} / c_p ratio increases from 0.0085 (0.85%) in late May, peaking at
602 nearly 0.012 (1.2%) in early August, and then decreasing back to 0.0085 (0.85%) in
603 September (Fig. 9b). The tendency towards a ratio of 1% in the core of the oligotrophic
604 season, evidences the increased proportion of nonalgal particles to the bulk pool as previously
605 observed in oligotrophic environments (Yentsch & Phinney 1989; Stramski et al. 2004; Loisel
606 et al. 2007).

607 The c_p and b_{bp} to Chl ratios exhibit not only different temporal patterns between the
608 Ligurian and Ionian Sea SCMs, they also exhibit different relative values. The c_p / Chl ratio in
609 the Ligurian Sea SCM is higher than that of the Ionian Sea, ranging from 0.18 to 0.45 m^2 mg
610 Chl^{-1}, compared to 0.15 to 0.26 m^2 mg Chl^{-1}, respectively. In contrast, although the b_{bp} / Chl
611 ratio in the Ligurian Sea SCM ranges from 0.0011 to 0.0023 m^2 mg Chl^{-1}, and the Ionian Sea
612 from 0.0015 to 0.0021 m^2 mg Chl^{-1}, they have essentially identical mean values over the time
613 series (0.0017±0.0006 and 0.0017±0.0001, respectively). This suggests that the POC in the
614 smaller size fractions are more similar in their respective SCM than in their larger size
615 fractions.

https://doi.org/10.5194/bg-2021-123
Preprint. Discussion started: 18 May 2021

616 Temporally, the Ligurian Sea SCM exhibits significantly more temporal variations in both
617 ratios compared to the Ionian Sea SCM, and the temporal variations are highly correlated.
618 Both the c_p / Chl and b_{bp} / Chl ratios in the Ligurian Sea SCM exhibit a peak at the start of the
619 time series in late May that decreases to mid-July, followed by a second peak during the
620 period coinciding with the production episode from mid-July to mid-August, and then a third
621 increase until the end of the time series (Figs. 9b–c). In contrast, both ratios in the Ionian Sea
622 SCM exhibit significantly reduced temporal variability (Figs. 9e–f), with a weak increase is
623 observed starting in early August.

624 Despite differing temporal variability, the b_{bp} / Chl ratio in both Seas remains moderate to
625 low (<0.0025 m^2 mg Chl^{-1}; Figs. 9c and 9f, consistent with global SCM values (Barbieux et
626 al., 2018). The enhanced b_{bp} / Chl values observed in the Ligurian Sea SCM in early May, late
627 July and late August suggest an increased contribution of small (pico- and nano-sized)
628 phytoplankton (Cetinić et al. 2012; Cetinić et al. 2015). Yet, the BOUSSOLE pigment data do
629 not reveal pronounced changes in the phytoplankton assemblage. Low-light conditions
630 typically prevailing in the SCM layer are usually associated with low values of the c_p / Chl
631 and b_{bp} / Chl ratios (e.g. (Behrenfeld & Boss 2003; Westberry et al., 2008; Barbieux et al.
632 2019), caused by photoacclimation by which phytoplankton organisms increase their
633 intracellular Chl. Nevertheless, the temporal variability in the c_p / Chl and b_{bp} / Chl values
634 may be resulting from fluctuations in the light conditions at the SCM in the Ligurian Sea. In
635 the Ionian Sea, the invariant low c_p / Chl and b_{bp} / Chl values are consistent with both
636 photoacclimation of phytoplankton to low-light conditions and a diatom-dominated
637 phytoplankton assemblage (Cetinić et al. 2015; Barbieux et al. 2018). The relatively stable
638 ratios observed in this region suggest a relative steadiness in the composition of the
639 phytoplankton assemblage over the considered period.

https://doi.org/10.5194/bg-2021-123
Preprint. Discussion started: 18 May 2021

640 **3.4.2 Relation to abiotic conditions**

641 The Ligurian Sea exhibits enhanced community production during the period from mid-
642 July to mid-August 2014, which is associated with a comparatively moderate increase in the
643 biomass indicators (Figs. 3–4) and c_p-derived POC (Fig. 7a). During this time period, the
644 depth of the SCM shoals by 25 m. This change occurs concurrently with a slight shoaling of
645 the density isopycnals (Figs. 3a–c), and a doubling (from 0.5 to 1 mol quanta m^{-2} d^{-1}) in the
646 daily PAR within the SCM layer (Fig. 10a). Therefore, we suggest that the observed
647 production episode may result from physical forcing that induces an upwelling of the water
648 mass, thereby resulting in an alleviation of the light/nutrient limitation and an adequate
649 balance between light and nutrient availability in the SCM layer. This SCM production
650 episode is associated with a moderate phytoplankton biomass (0.8 Chl mg m^{-3}), dominated by
651 a nanoplankton community. It coincides with an increase in the c_p / Chl and b_{bp} / Chl ratios,
652 which we attribute to a boost in the carbon-to-Chl ratio resulting from production in enhanced
653 light conditions. Because it appears to result from changes in light conditions, we may
654 attribute this production event to phytoplankton (not community) growth.

655 In the Ionian Sea, the depth of the SCM follows the depth of the isopycnal 28.85 during
656 the period from late to May to mid-August 2017 (Figs. 3d–f). In mid-August, the SCM
657 reaches its deepest point (~125 m) concurrent with deepening isopycnals, decreased PAR
658 levels within the SCM layer (Fig. 10b) and minimum values of Chl, c_p and b_{bp}. Afterwards,
659 the SCM depth decouples from the position of the isopycnals (Fig. 3d–f), the SCM becomes
660 shallower and the mean daily PAR in the SCM layer increases. Nevertheless, the observed
661 temporal fluctuations in the abiotic forcing and biological indicators do not seem to relate
662 with any clear change in the community production (Figs. 7d–f). This suggests that physics-
663 induced changes in the position of the SCM are not sufficient to alleviate the light and/or
664 nutrient limitation occurring at this time in the considered area (Guieu et al. 2020).

https://doi.org/10.5194/bg-2021-123
Preprint. Discussion started: 18 May 2021

665 Considering the large contribution of diatoms at the SCM, one may conclude that the low, yet
666 non-negligible, production levels estimated in the SCM layer are supported by diatoms. This
667 result supports previous findings indicating that, contrary to the classic view of diatoms
668 thriving essentially in dynamic eutrophic conditions, these organisms have the ability to
669 maintain in stratified oligotrophic environments, including in deep layers under low light-
670 nutrient conditions (Kemp & Villareal 2013; Kemp & Villareal, 2018).

671 **3.5 Contribution of the SCM to the water column production**

672 In order to assess the relative contribution of the SCM layer to the production occurring
673 in the whole water column, we compare the c_p-based estimates integrated within the
674 productive layer (0–1.5 Z_{eu}) and SCM layers. Our results suggest that, for these oligotrophic
675 systems, the production integrated within the SCM layer represents a substantial fraction
676 (F_{SCM}) of the gross community production integrated within the productive layer. This is
677 particularly the case for the Ligurian Sea where F_{SCM} reaches ~42%, and to a lesser extent for
678 the Ionian Sea with F_{SCM} ~16%.

679 Subtropical stratified oligotrophic gyres cover 45% of the global ocean (McClain et al.
680 2004). Assuming that the Ionian Sea is representative of such systems (e.g. Mignot et al.
681 2014; Barbieux et al. 2019), and extrapolating the estimated relative contribution of the SCM
682 layer to the water column production in the Ionian (F_{SCM} ~16%), then the SCM layer would
683 contribute ~7% of the community production of the water column on a global scale (i.e. F_{SCM}
684 of 16% multiplied by a global spatial occurrence of 45%). In addition, using a global BGC-
685 Argo database, Cornec et al. (2021) estimated that SCMs in oligotrophic subtropical gyres
686 behave as SBM 8–42% of the year, depending on the season. Thus, assuming the Ligurian
687 SCM oligotrophic summer system as a reference for SBM, the contribution of the SCM layer
688 to the global water column production could seasonally reach 19% (i.e. F_{SCM} of 42%
689 multiplied by a global spatial occurrence of 45%).

https://doi.org/10.5194/bg-2021-123
Preprint. Discussion started: 18 May 2021

690 We recognize that these estimates are very crude and need to be refined and confirmed
691 in future studies. Yet they suggest that the contribution of the SCM layer to the water column
692 production may be significant globally, although commonly ignored. Our observations are
693 consistent with previous findings (Crombet et al. 2011; Kemp & Villareal 2013; Mignot et al.
694 2014), and suggest that stratified oligotrophic systems should no longer be considered as
695 steady oceanic deserts and that their biogeochemical contribution should be accounted for and
696 better quantified to improve global carbon budgets.

697 **4 Conclusions**

698 The present study represents a first attempt to apply the bio-optical diel cycle-based
699 method (Siegel et al. 1989; Claustre et al. 2008) to the c_p and b_{bp} coefficients measured by
700 two BGC-Argo profiling floats. It aims to quantify gross community production in different
701 layers of the water column, the subsurface chlorophyll maximum (SCM) layer in particular,
702 during the oligotrophic summer season in two distinct systems of the Mediterranean, i.e. the
703 Ligurian Sea and the Ionian Sea.

704 From a methodological point of view, our results indicate that, compared to the c_p
705 coefficient, the diel cycle of the b_{bp} coefficient is not an optimal proxy for the daily POC
706 variations, so that we are not confident using the b_{bp}-based gross community production
707 estimates, although it may provide a more robust proxy for the fraction of particulate matter in
708 the smaller size classes. Our results for the surface layer of the Ligurian Sea are consistent
709 with previous studies from moored observations (Kheireddine & Antoine 2014; Barnes &
710 Antoine 2014), and we found they are valid for the entire water column and for both the
711 Ligurian and Ionian Seas. These results have major implications for use of the methodology
712 with geostationary ocean color missions and standard BGC-Argo profiling floats that yield
713 only the b_{bp} coefficient. The present results thus argue in favor of a frequent implementation

https://doi.org/10.5194/bg-2021-123
Preprint. Discussion started: 18 May 2021

714 onto BGC-Argo floats of transmissometers (c_p sensors), which provide information on a suite
715 of key biogeochemical variables (Claustre et al. 2020), from phytoplankton community
716 composition (Rembauville et al. 2017), to particle flux export (Briggs et al. 2011; Estapa et al.
717 2013) and, as demonstrated here, biological production (White et al. 2017; Briggs et al. 2018).

718 Our c_p-based gross community production rates compare consistently with previous
719 estimates from a similar approach applied to oligotrophic waters (Claustre et al. 2008; Gernez
720 et al. 2011; Barnes & Antoine 2014). These values are also consistent with estimates of
721 primary production either computed from the model of Morel (1991) coupled to the
722 considered BGC-Argo data, or published in the literature, although admittedly higher. This is
723 unsurprising because the present estimates are based on the c_p coefficient, which accounts for
724 both autotrophic and heterotrophic organisms (not just phytoplankton). This nevertheless
725 raises the question of the selection of an empirical bio-optical relationship, which is key to
726 converting c_p into POC equivalent. In the present study, the c_p-derived production estimates
727 on average decrease by 25% or increase by 37% depending on the used bio-optical
728 relationship, which is not negligible. Hence, we recommend POC sampling simultaneously to
729 BGC-Argo floats deployment. This will help to better constrain bio-optical relationships and
730 ultimately improve the reliability of the biomass and production estimates.

731 Our results indicate that both the Ligurian and Ionian Seas may sustain relatively large
732 levels of gross community production during the oligotrophic summer period, with a
733 substantial contribution by the SCM layer, a feature characteristic of oligotrophic systems that
734 is typically considered as steady and non-productive. In the Ligurian, the SCM behaves as a
735 subsurface biomass maximum (SBM) and appears to respond to episodic abiotic forcing, with
736 increased production rates coinciding with enhanced light availability in response to shoaling
737 isopycnals and SCM. In this system, the particle assemblage is dominated by phytoplankton
738 organisms, mainly nanoflagellates. In contrast, the Ionian SCM layer essentially reflects

https://doi.org/10.5194/bg-2021-123
Preprint. Discussion started: 18 May 2021

739 photoacclimation of phytoplankton cells to prevailing environmental conditions. It does not
740 seem affected by modifications in abiotic forcing, although the phytoplankton assemblage
741 appears to be dominated by diatoms. These results agree with previous BGC-Argo-based
742 studies describing the occurrence and functioning of SCM systems in the global ocean
743 (Mignot et al. 2014; Cornec et al. 2021) and Mediterranean Sea (Lavigne et al. 2015;
744 Barbieux et al. 2019), and offer a first attempt to quantify biological production in such
745 systems. More generally, our study suggests that the contribution of the SCM layer to the
746 water column production varies broadly depending the considered system, whether seasonally
747 (~42% in the Ligurian Sea) or permanently (~16% in the Ionian Sea) oligotrophic.

748 Our study emphases the promising potential of BGC-Argo profiling floats for providing
749 a non-intrusive, high-frequency assessment of POC production within the whole water
750 column, which is critical in particular for applications to stratified oligotrophic environments
751 with recurring or permanent SCMs. The present results, based on data from two
752 Mediterranean environments, should be confirmed in the future through the deployment of
753 "multi-profiling" BGC-Argo floats in the broad, remote subtropical gyres. In such systems,
754 biological production is not constant but, instead, shows high temporal heterogeneity (Karl et
755 al. 2003; Claustre et al. 2008) that may be missed by traditional sampling, leading to a
756 potential underestimate of the biogeochemical impact of these systems in global carbon
757 budgets. Implementing such a BGC-Argo-based approach to carbon flux quantification
758 becomes even more important in the perspective of climate change, which is predicted to
759 induce an expansion of stratified oligotrophic gyres and an oligotrophication of the oceans
760 (Sarmiento et al. 2004) as already observed from satellite imagery (Polovina et al. 2008;
761 Signorini et al. 2015).

762

https://doi.org/10.5194/bg-2021-123
Preprint. Discussion started: 18 May 2021

763 *Author contribution* MB, JU and AB designed the work and prepared the manuscript. MB
764 processed the data and conducted the analyses. MB, JU and CR prepared the plots. AM and
765 BG developed the biological production model. AM helped with the implementation of the
766 model and the interpretation of the ouput data. CR contributed to the analysis of the diel bio-
767 optical variability, interpretation of bio-optical data and the organization of the manuscript.
768 HC contributed to the interpretation of the BGC-Argo data and biological production. HL
769 helped with the interpretation of the bio-optical data and the global extrapolation of the
770 results. VT and FDO contributed to the BGC-Argo float deployments and interpretation of the
771 physical data. AP prepared and tested the BGC-Argo floats prior to deployment and set up the
772 raw data stream. EL and CP developed the BGC-Argo float version used in this study and
773 contributed to float preparation. CS handled BGC-Argo data archiving and distribution. All
774 authors reviewed and approved the manuscript.

775

776 *Data availability* The BGC-Argo profiling float data and metadata used in this paper may
777 be downloaded from the Argo GDAC (http://doi.org/10.17882/42182). All other original data
778 are available from the Argo Global Data Assembly Center (ftp://ftp.ifremer.fr/ifremer/argo).
779 These data were collected and made freely available by the International Argo Program and
780 the national programs that contribute to it (http://www.argo.ucsd.edu; https://www.ocean-
781 ops.org). The Argo Program is part of the Global Ocean Observing System. The
782 PEACETIME project pigment data are available from the SEANOE archive under the
783 following reference: Guieu et al., Biogeochemical dataset collected during the PEACETIME
784 cruise, SEANOE, https://doi.org/10.17882/75747, 2020. The BOUSSOLE program pigment
785 data may be accessed upon request (http://www.obs-
786 vlfr.fr/Boussole/html/boussole_data/login_form.php).

787

https://doi.org/10.5194/bg-2021-123
Preprint. Discussion started: 18 May 2021

Acknowledgement This paper represents a contribution to the following projects: PEACETIME (https://doi.org/10.17600/17000300), a joint initiative of the MERMEX and ChArMEx components supported by CNRS-INSU, IFREMER, CEA, and Météo-France as part of the program MISTRALS coordinated by INSU; PEACETIME-OC supported by the French program CNES-TOSCA; remOcean funded by ERC (grant 246777); and NAOS funded by ANR Equipex (grant J11R107-F). MB was funded by a PhD grant from Sorbonne Université (Ecole Doctorale 129). Phytoplankton pigment analyses were performed at the SAPIGH national HPLC analytical service at the Institut de la Mer de Villefranche (IMEV). We acknowledge the captains and crew of the Téthys and Pourquoi Pas? research vessels during the BOUSSOLE and PEACETIME cruises, as well as David Antoine, PI of the BOUSSOLE project, and Cécile Guieu and Karine Desboeufs, PIs of the PEACETIME project. We thank the International Argo Program and Coriolis project, which contributed to making the data freely and publicly available. Marin Cornec is also warmly thanked for useful discussion regarding biological production in SCM systems.

References

Ahn, Y.-H., Bricaud, A., and Morel, A.: Light backscattering efficiency and related properties of some phytoplankters, Deep-Sea Res. Pt. A, 39, 1835–1855, https://doi.org/10.1016/0198-0149(92)90002-B, 1992.

Allen, J.I., Somerfield, P.J., and Siddorn, J.: Primary and bacterial production in the Mediterranean Sea: a modelling study, J. Mar. Syst., 33–34, 473–495, https://doi.org/10.1016/S0924-7963(02)00072-6, 2002.

Álvarez, E., Morán, X. A. G., López-Urrutia, Á., and Nogueira, E.: Size-dependent photoacclimation of the phytoplankton community in temperate shelf waters (southern

https://doi.org/10.5194/bg-2021-123
Preprint. Discussion started: 18 May 2021

812 Bay of Biscay), Mar. Ecol. Prog. Ser., 543, 73–87, https://doi.org/10.3354/meps11580,
813 2016.

814 Antoine, D., Morel, A., and André, J.-M.: Algal pigment distribution and primary production
815 in the eastern Mediterranean as derived from coastal zone color scanner observations, J.
816 Geophys. Res, 100, 16193–16209, https://doi.org/10.1029/95JC00466, 1995.

817 Antoine, D. André, J.-M, and Morel, A.: Oceanic primary production: 2. Estimation at global
818 scale from satellite (Coastal Zone Color Scanner) chlorophyll, Global Biogeochem. Cy.,
819 10, 57–69, https://doi.org/10.1029/95GB02832, 1996.

820 Antoine, D., D'Ortenzio, F., Hooker, S. B., Bécu, G., Gentili, B., Tailliez, D., and Scott, A. J.:
821 Assessment of uncertainty in the ocean reflectance determined by three satellite ocean
822 color sensors (MERIS, SeaWiFS and MODIS-A) at an offshore site in the
823 Mediterranean Sea (BOUSSOLE project), J. Geophys. Res., 113, 1–22,
824 https://doi.org/10.1029/2007JC004472, 2008.

825 Barber, R. T., and Hitling, A. K.: History of the study of plankton productivity, in:
826 Phytoplankton Productivity: Carbon assimilation in marine and freshwater ecosystems,
827 edited by Williams, P. J. le B., Thomas, D. N., and Reynolds, C. S., Blackwell Science,
828 Oxford, 16–43, https://doi.org/10.1002/9780470995204, 2002.

829 Barbieux, M., Uitz, J., Bricaud, A., Organelli, E., Poteau, A., Schmechtig, C., Gentili, B.,
830 Penkerc'h, C., Leymarie, E., D'Ortenzio, F., and Claustre, H.: Assessing the variability
831 in the relationship between the particulate backscattering coefficient and the chlorophyll
832 a concentration from a global Biogeochemical-Argo database, J. Geophys. Res., 123,
833 1229–1250, https://doi.org/10.1002/2017JC013030, 2017.

834 Barbieux, M., Uitz, J., Gentili, B., Pasqueron de Fommervault, O., Mignot, A., Poteau, A.,
835 Schmechtig, C., Taillandier, V., Leymarie, E., Penkerc'h, C., D'Ortenzio, F., Claustre,

836 H., and Bricaud, A.: Bio-optical characterization of subsurface chlorophyll maxima in
837 the Mediterranean Sea from a Biogeochemical-Argo float database, Biogeosciences, 16,
838 1321–1342, https://doi.org/10.5194/bg-16-1321-2019, 2019.

839 Barnes, M., and Antoine, D.: Proxies of community production derived from the diel
840 variability of particulate attenuation and backscattering coefficients in the northwest
841 mediterranean sea, Limnol. Oceanogr., 59, 2133–2149,
842 https://doi.org/10.4319/lo.2014.59.6.2133, 2014.

843 Beckmann, A. and Hense, I.: Beneath the surface: Characteristics of oceanic ecosystems
844 under weak mixing conditions – A theoretical investigation, Prog. Oceanogr., 75, 771–
845 796, https://doi.org/10.1016/j.pocean.2007.09.002, 2007.

846 Behrenfeld, M. J., and Boss, E.: The beam attenuation to chlorophyll ratio: an optical index of
847 phytoplankton physiology in the surface ocean?, Deep-Sea Res. Pt. I, 50, 1537–1549,
848 https://doi.org/10.1016/j.dsr.2003.09.002, 2003.

849 Behrenfeld, M. J., and Boss, E.: Beam attenuation and chlorophyll concentration as
850 alternative optical indices of phytoplankton biomass, J. Mar. Res., 64, 431–451,
851 https://doi.org/10.1357/002224006778189563, 2006.

852 Behrenfeld, M. J., Marañón, E., Siegel, D. A., and Hooker, S. B.: Photoacclimation and
853 nutrient-based model of light-saturated photosynthesis for quantifying oceanic primary
854 production, Mar. Ecol. Prog. Ser., 228, 103–117, https://doi.org/10.3354/meps228103,
855 2002.

856 Bernard, S., Probyn, T. A., and Quirantes, A.: Simulating the optical properties of
857 phytoplankton cells using a two-layered spherical geometry, Biogeosciences Discuss.,
858 6, 1497–1563, https://doi.org/10.5194/bgd-6-1497-2009, 2009.

https://doi.org/10.5194/bg-2021-123
Preprint. Discussion started: 18 May 2021

859 Bethoux, J. P., Morin, P., Madec, C., and Gentili, B.: Phosphorus and nitrogen behaviour in
860 the Mediterranean Sea, Deep-Sea Res., 39, 1641–1654, https://doi.org/10.1016/0198-
861 0149(92)90053-V, 1992.

862 Bosc, E., Bricaud, A., and Antoine, D.: Seasonal and interannual variability in algal biomass
863 and primary production in the Mediterranean Sea, as derived from 4 years of SeaWiFS
864 observations, Global Biogeochem. Cy. 18, GB1005,
865 https://doi.org/10.1029/2003GB002034, 2004.

866 Boss, E., Pegau, W. S., Lee, M., Twardowski, M., Shybanov, E., Korotaev, G., and
867 Baratange, F.: Particulate backscattering ratio at LEO 15 and its use to study particle
868 composition and distribution, J. Geophys. Res., 109, C01014,
869 https://doi.org/10.1029/2002JC001514, 2004.

870 Boss., E., and Zaneveld, J. R. V.: The effect of bottom substrate on inherent optical
871 properties: Evidence of biogeochemical processes. Limnol. Oceanogr., 48, 346–354.
872 https://doi.org/10.4319/lo.2003.48.1_part_2.0346, 2003.

873 Bricaud, A., Morel, A., and Prieur, L.: Absorption by dissolved organic matter of the sea
874 (yellow substance) in the UV and visible domains, Limnol. Oceanogr., 26,
875 https://doi.org/10.4319/lo.1981.26.1.0043, 1981.

876 Briggs, N., Perry, M. J., Cetinić, I., Lee, C., D'Asaro, E., Gray, A. M., Rehm, E.: High-
877 resolution observations of aggregate flux during a sub-polar North Atlantic spring
878 bloom, Deep-Sea Res. Pt. I, 58, 1031–1039, https://doi.org/10.1016/j.dsr.2011.07.007,
879 2011.

880 Briggs, N., Guðmundsson, K., Cetinić, I., D'Asaro, E., Rehm, E., Lee, C., and Perry, M. J.: A
881 multi-method autonomous assessment of primary productivity and export efficiency in

https://doi.org/10.5194/bg-2021-123
Preprint. Discussion started: 18 May 2021

882 the springtime North Atlantic, Biogeosciences, 15, 4515–4532,
883 https://doi.org/10.5194/bg-15-4515-2018, 2018.

884 Brunet C., Casotti R., Vantrepotte V., and Conversano F.: Vertical variability and diel
885 dynamics of picophytoplankton in the Strait of Sicily, Mediterranean Sea, in summer,
886 Mar. Ecol. Prog. Ser., 346, 15–26, https://doi.org/10.3354/meps07017, 2007.

887 Casotti, R., Landolfi, A., Brunet, C., D'Ortenzio, F., Mangoni, O., and Ribera d'Alcalá, M.:
888 Composition and dynamics of the phytoplankton of the Ionian Sea (eastern
889 Mediterranean), J. Geophys. Res., 108, 1–19, https://doi.org/10.1029/2002JC001541,
890 2003.

891 Cetinić, I., Perry, M. J., Briggs, N. T., Kallin, E., D'Asaro, E. A., and Lee, C. M.: Particulate
892 organic carbon and inherent optical properties during 2008 North Atlantic Bloom
893 Experiment, J. Geophys. Res., 117, 1–18, https://doi.org/10.1029/2011JC007771, 2012.

894 Cetinić, I., Perry, M. J., D'Asaro, E., Briggs, N., Poulton, N., Sieracki, M. E., and Lee, C. M.:
895 A simple optical index shows spatial and temporal heterogeneity in phytoplankton
896 community composition during the 2008 North Atlantic Bloom Experiment,
897 Biogeosciences, 12, 2179–2194, https://doi.org/10.5194/bg-12- 2179-2015, 2015.

898 Chavez F. P., Messié, M., and Pennington, J. T.: Marine Primary Production in Relation to
899 Climate Variability and Change, Annual Rev. Mar. Sci., 3, 227–260,
900 https://doi.org/10.1146/annurev.marine.010908.163917, 2013.

901 Claustre, H.: The trophic status of various oceanic provinces as revealed by phytoplankton
902 pigment signatures, Limnol. Oceanogr., 39, 1206–1210, 39,
903 https://doi.org/10.4319/lo.1994.39.5.1206, 2014.

https://doi.org/10.5194/bg-2021-123
Preprint. Discussion started: 18 May 2021

904 Claustre, H., Bricaud, A., Babin, M., Bruyant, F., Guillou, L., Le Gall, F., Marie, D.,
905 Partensky, F.: Diel variations in Prochlorococcus optical properties, Limnol. Oceanogr.,
906 47, 1637–1647, https://doi.org/10.4319/lo.2002.47.6.1637, 2002.

907 Claustre, H., Huot, Y., Obernosterer, I., Gentili, B., Tailliez, D., and Lewis, M.: Gross
908 community production and metabolic balance in the South Pacific Gyre, using a non
909 intrusive bio-optical method, Biogeosciences, 5, 463–474, https://doi.org/10.5194/bg-5-
910 463-2008, 2008.

911 Cloern, J. E.: The relative importance of light and nutrient limitation of phytoplankton
912 growth: A simple index of coastal ecosystem sensitivity to nutrient enrichment, Aquat.
913 Ecol., 33, 3–16, https://doi.org/10.1023/A:1009952125558, 1999.

914 Cornec, M., Claustre, H., Mignot, A., Guidi, L., Lacour, L., Poteau, A., D'Ortenzio, F.,
915 Gentili, B., and Schmechtig, C.: Deep chlorophyll maxima in the global ocean:
916 occurrences, drivers and characteristics, Global Biogeochem. Cy., 35, e2020GB006759,
917 https://doi.org/10.1029/2020GB006759, 2021.

918 Crombet, Y., Leblanc, K., Quéguiner, B., Moutin, T., Rimmelin, P., Ras, J., Claustre, H.,
919 Leblond, N., Oriol, L., and Pujo-Pay, M.: Deep silicon maxima in the stratified
920 oligotrophic Mediterranean Sea, Biogeosciences, 8, 459–475,
921 https://doi.org/10.5194/bg-8-459-2011, 2011.

922 Cullen, J. J.: The deep chlorophyll maximum: comparing vertical profiles of chlorophyll a,
923 Can. J. Fish. Aquat. Sci., 39, 791–803, https://doi.org/10.1139/f82-108, 1982.

924 Cullen, J. J., Lewis, M. R., Davis, C. O., and Barber, R. T.: Photosynthetic characteristics and
925 estimated growth rates indicate grazing is the proximate control of primary production
926 in the equatorial Pacific, J. Geophys. Res., 97, 639–654,
927 https://doi.org/10.1029/91JC01320, 1992.

https://doi.org/10.5194/bg-2021-123
Preprint. Discussion started: 18 May 2021

928 Cullen, J. J., and Lewis, M. R.: Biological processes and optical measurements near the sea
929 surface: Some issues relevant to remote sensing, J. Geophys. Res., 100(C7), 13255–
930 13266, https://doi.org/10.1029/95JC00454, 1995.

931 Cullen, J. J.: Subsurface chlorophyll maximum layers: enduring enigma or mystery solved?,
932 Ann Rev Mar Sci., 7, 207-39, https://doi.org/10.1146/annurev-marine-010213-135111,
933 2015.

934 Dandonneau, Y.: Measurement of in situ profiles of primary production using an automated
935 sampling and incubation device, ICES Mar. Sci. Sym., 197, 172–180, 1993.

936 de Boyer Montégut, C., Madec, G., Fischer, A. S., Lazar, A., and Iudicone, D.: Mixed layer
937 depth over the global ocean: An examination of profile data and a profile-based
938 climatology, J. Geophys. Res., 109, 1–20, https://doi.org/10.1029/2004JC002378, 2004.

939 del Giorgio P. A., and Duarte C. M.: Respiration in the open ocean, Nature, 420, 37984.
940 https://doi.org/10.1038/nature01165, 2002.

941 Di Cicco, A., Sammartino, M, Marullo, S., and Santoleri, R.: Regional empirical algorithms
942 for an improved identification of phytoplankton functional types and size classes in the
943 Mediterranean Sea using satellite data, Frontiers Mar. Sci., 4126, 1–18, https://doi.org/
944 10.3389/fmars.2017.00126, 2017.

945 D'Ortenzio, F. and Ribera d'Alcalà, M.: On the trophic regimes of the Mediterranean Sea: a
946 satellite analysis, Biogeosciences, 6, 139–148, https://doi.org/10.5194/bg-6-139-2009,
947 2009.

948 Duarte, C. M., and Agusti S.: The CO_2 balance of unproductive aquatic ecosystems, Science,
949 281, 234–6, https://doi.org/10.1126/science.281.5374.234, 1998.

https://doi.org/10.5194/bg-2021-123
Preprint. Discussion started: 18 May 2021

950 Dubinsky, Z., and Stambler, N.: Photoacclimation processes in phytoplankton: mechanisms,
951 consequences, and applications, Aquat. Microb. Ecol., 56,163–176,
952 https://doi.org/10.3354/ame01345, 2009.

953 Dugdale, R. C., and Wilkerson, F. P.: Nutrient sources and primary production in the Eastern
954 Mediterranean, Oceanologica Acta, 1988.

955 Durand, M. D., and Olson, R. J.: Contributions of phytoplankton light scattering and cell
956 concentration changes to diel variations in beam attenuation in the equatorial pacific
957 from flow cytometric measurements of pico-, ultra and nanoplankton, Deep-Sea Res. Pt.
958 II, 43, 891–906, https://doi.org/10.1016/0967-0645(96)00020-3, 1996.

959 Durand, M. D., and Olson, R.J.: Diel patterns in optical properties of the chlorophyte
960 Nannochloris sp.: Relating individual-cell to bulk measurements, Limnol. Oceanogr.,
961 43, 1107–1118, https://doi.org/10.4319/lo.1998.43.6.1107, 1998.

962 Durand, M. D. Green, R. E., Sosik, H. M. and Olson, R. J.: Diel Variations in Optical
963 Properties of Micromonas Pusilla (Prasinophyceae), J. Phycol., 38, 1132–1142,
964 https://doi.org/10.1046/j.1529-8817.2002.02008.x, 2002.

965 Estapa, M. L., Buesseler, K., Boss, E., and Gerbi, G.: Autonomous, high-resolution
966 observations of particle flux in the oligotrophic ocean, Biogeosciences, 10, 5517–5531,
967 https://doi.org/10.5194/bg-10-5517-2013, 2013.

968 Falkowski, P. G.: Ocean Science: The power of plankton, Nature, 483**,** S17–S20,
969 https://doi.org/10.1038/483S17a, 2012.

970 Fennel, K., and Boss, E.: Subsurface maxima of phytoplankton and chlorophyll: Steady-state
971 solutions from a simple model, Limnol. Oceanogr., 48, 1521–1534,
972 https://doi.org/10.4319/lo.2003.48.4.1521, 2003.

https://doi.org/10.5194/bg-2021-123
Preprint. Discussion started: 18 May 2021

973 Field, C. B., Behrenfeld, M. J., Randerson, J. T., and Falkowski, P.: Primary production of the
974 biosphere: integrating terrestrial and oceanic components, Science 281, 237–240,
975 https://doi.org/10.1126/science.281.5374.237, 1998.

976 Fitzwater, S.E., Knauer, G.A., and Martin, J.H.: Metal contamination and its effect on primary
977 production measurements, Limnol. Oceanogr., 27, 44–551,
978 https://doi.org/10.4319/lo.1982.27.3.0544, 1982.

979 Gardner, W. D., Mishonov, A. V., and Richardson, M. J.: Global POC concentrations from
980 in-situ and satellite data, Deep-Sea Res. Pt. II, 53, 718-740,
981 https://doi.org/10.1016/j.dsr2.2006.01.029, 2006.

982 Geider, R. J.: Light and temperature dependence of the carbon to chlorophyll a ratio in
983 microalgae and cyanobacteria: Implications for physiology and growth of
984 phytoplankton, New Phytol., 106, 1–34, https://doi.org/10.1111/j.1469-
985 8137.1987.tb04788.x, 1987.

986 Geider, R. J., MacIntyre, H. L., and Kana T. M.: Dynamic model of phytoplankton growth
987 and acclimation: Responses of the balanced growth rate and the chlorophyll a:carbon
988 ratio to light, nutrient-limitation and temperature, Mar. Ecol. Prog. Ser., 148, 187–200,
989 https://doi.org/10.3354/meps148187, 1997.

990 Gernez, P., Antoine, D., and Huot, Y.: Diel cycles of the particulate beam attenuation
991 coefficient under varying trophic conditions in the northwestern Mediterranean Sea:
992 Observations and modeling, Limnol. Oceanogr., 56, 17–36,
993 https://doi.org/10.4319/lo.2011.56.1.0017, 2011.

994 Gitelson, A., Karnieli, A., Goldman, N., Yacobi, Y.Z., and Mayo, M.: Chlorophyll estimation
995 in the Southeastern Mediterranean using CZCS images: adaptation of an algorithm and

its validation, J. Mar. Syst., 9, 283–290, https://doi.org/10.1016/S0924-7963(95)00047-X, 1996.

Guieu, C., D'Ortenzio, F., Dulac, F., Taillandier, V., Doglioli, A., Petrenko, A., Barrillon, S., Mallet, M., Nabat, P., and Desboeufs, K.: Introduction: Process studies at the air–sea interface after atmospheric deposition in the Mediterranean Sea – objectives and strategy of the PEACETIME oceanographic campaign (May–June 2017), Biogeosciences, 17, 5563–5585, https://doi.org/10.5194/bg-17-5563-2020, 2020.

González, N., Anadón, R., Mouriño, B., Fernández, E., Sinha, B., Escánez, J., and de Armas, D.: The metabolic balance of the planktonic community in the North Atlantic Subtropical Gyre: The role of mesoscale instabilities, Limnol. Oceanogr., 4, https://doi.org/10.4319/lo.2001.46.4.0946, 2001.

González, N., Anadón, R., and Marañón, E.: Large-scale variability of planktonic net community metabolism in the Atlantic Ocean: Importance of temporal changes in oligotrophic subtropical waters, Mar. Ecol. Progr. Ser., 233, 21–30, https://doi.org/10.3354/meps233021, 2002.

Gordon, H. R., and McCluney, W. R.: Estimation of the Depth of Sunlight Penetration in the Sea for Remote Sensing, Appl. Opt., 14, 413–416, https://doi.org/10.1364/AO.14.000413, 1975.

Hense, I., and Beckmann, A.: Revisiting subsurface chlorophyll and phytoplankton distributions, Deep-Sea Res. Pt. I, 55, 1193–1199, https://doi.org/10.1016/j.dsr.2008.04.009, 2008.

Jacquet, S., Lennon, J.-F., Marie, D., and Vaulot, D.: Picoplankton population dynamics in coastal waters of the northwestern Mediterranean Sea, Limnol. Oceanogr., 43, 1916–1931, https://doi.org/10.4319/lo.1998.43.8.1916, 1998.

https://doi.org/10.5194/bg-2021-123
Preprint. Discussion started: 18 May 2021

1020 Juranek, L. W., and Quay, P. D.: In vitro and in situ gross primary and net community
1021 production in the North Pacific Subtropical Gyre using labeled and natural abundance
1022 isotopes of dissolved O_2, Glob. Biogeochem. Cy., 19,
1023 https://doi.org/10.1029/2004GB002384, 2005.

1024 Karl, D. M., Laws, E. A., Morris, P., Williams, P. J. le B, and Emerson, S.: Metabolic balance
1025 of the open sea, Nature, 426, 32–32, https://doi.org/10.1038/426032a, 2003.

1026 Kemp, A. E. S., and Villareal, T. A.: High diatom production and export in stratified waters -
1027 A potential negative feedback to global warming, Prog. Oceanogr., 119, 4–23,
1028 https://doi.org/10.1016/j.pocean.2013.06.004, 2013.

1029 Kemp, A. E. S., and Villareal, T. A.: The case of the diatoms and the muddled mandalas:
1030 Time to recognize diatom adaptations to stratified waters, Prog. Oceanogr., 167, 138-
1031 149, https://doi.org/10.1016/j.pocean.2018.08.002, 2018.

1032 Kheireddine, M., and Antoine, D.: Diel variability of the beam attenuation and backscattering
1033 coefficients in the northwestern Mediterranean Sea (BOUSSOLE site), J. Geophys.
1034 Res., 119, 5465– 5482, https://doi.org/10.1002/2014JC010007, 2014.

1035 Kiefer, D. A., Olson, R. J., and Holm-Hansen, O.: Another look at the nitrite and chlorophyll
1036 maxima in the central North Pacific, Deep-Sea Res., 23, 1199–1208,
1037 https://doi.org/10.1016/0011-7471(76)90895-0, 1976.

1038 Lacroix, G., and Nival, P.: Influence of meteorological variability on primary production
1039 dynamics in the Ligurian Sea (NW Mediterranean Sea) with a 1D
1040 hydrodynamic/biological model, J. Mar. Syst., 16, 23–50,
1041 https://doi.org/10.1016/S0924-7963(97)00098-5, 1998.

1042 Lavigne, H., D'Ortenzio, F., Migon, C., Claustre, H., Testor, P., Ribera d'Alcalà, M., Lavezza,
1043 R., Houpert, L., and Prieur, L.: Enhancing the comprehension of mixed layer depth

1044 control on the Mediterranean phytoplankton phenology, J. Geophys. Res. Oceans, 118,
1045 3416–3430, https://doi.org/10.1002/jgrc.2025, 2013.

1046 Lavigne, H., D'Ortenzio, F., Ribera D'Alcalà, M., Claustre, H., Sauzède, R., and Gacic, M.:
1047 On the vertical distribution of the chlorophyll a concentration in the Mediterranean Sea:
1048 a basin-scale and seasonal approach, Biogeosciences, 12, 5021–5039,
1049 https://doi.org/10.5194/bg-12-5021-2015, 2015.

1050 Letelier, R. M., Karl, D. M., Abbott, M. R., Bidigare, R. R.: Light driven seasonal patterns of
1051 chlorophyll and nitrate in the lower euphotic zone of the North Pacific Subtropical
1052 Gyre, Limnol. Oceanogr., 2, 508–519, https://doi.org/10.4319/lo.2004.49.2.0508, 2004.

1053 Loisel, H., Mériaux, X., Berthon, J.-F., Poteau, A.: Investigation of the optical backscattering
1054 to scattering ratio of marine particles in relation to their biogeochemical composition in
1055 the eastern English Channel and southern North Sea, Limnol. Oceanogr., 52, 739–752,
1056 https://doi.org/10.4319/lo.2007.52.2.0739, 2007.

1057 Loisel, H., Vantrepotte, V., Norkvist, K., Mériaux, X., Kheireddine, M., Ras, J., Pujo-Pay, M.,
1058 Combet, Y., Leblanc, K., Dall'Olmo, G., Mauriac, R., Dessailly, D., and Moutin, T.:
1059 Characterization of the bio-optical anomaly and diurnal variability of particulate matter,
1060 as seen from scattering and backscattering coefficients, in ultra-oligotrophic eddies of
1061 the Mediterranean Sea, Biogeosciences, 8, 3295–3317, https://doi.org/10.5194/bg-8-
1062 3295-2011, 2011.

1063 Longhurst, A., Sathyendranath, S., Platt, T., and Caverhill, C.: An estimate of global primary
1064 production in the ocean from satelite radiometer data, J. Plank. Res., 17, 1245–1271,
1065 https://doi.org/10.1093/plankt/17.6.1245, 1995.

https://doi.org/10.5194/bg-2021-123
Preprint. Discussion started: 18 May 2021

1066 Magazzu, G., and Decembrini, F.: Primary production, biomass and abundance of
1067 phototrophic picoplankton in the Mediterranean Sea: A review, Aquat. Microb. Ecol., 9,
1068 97– 104, https://doi.org/10.3354/ame009097, 1995.

1069 Marañón, E., Van Wambeke, F., Uitz, J., Boss, E. S., Dimier, C., Dinasquet, J., Engel, A.,
1070 Haëntjens, N., Pérez-Lorenzo, M., Taillandier, V., and Zäncker, B.: Deep maxima of
1071 phytoplankton biomass, primary production and bacterial production in the
1072 Mediterranean Sea, Biogeosciences, 18, 1749–1767, https://doi.org/10.5194/bg-18-
1073 1749-2021, 2021.

1074 Marra, J., Langdon, C., and Knudson, C. A.: Primary production, water column changes, and
1075 the demise of a Phaeocystis bloom at the Marine Light-Mixed Layers site (59°N, 21°W)
1076 in the northeast Atlantic Ocean, J. Geophys. Res., 100, 6633–6643,
1077 https://doi.org/10.1029/94JC01127, 1995.

1078 Marty, J. C., Chiavérini, J., Pizay, M. D., and Avril, B.: Seasonal and interannual dynamics of
1079 nutrients and phytoplankton pigments in the western Mediterranean Sea at the
1080 DYFAMED time- series station (1991–1999), Deep-Sea Res. Pt. II, 49, 1965–1985,
1081 https://doi.org/10.1016/S0967-0645(02)00022-X, 2002.

1082 Marty, J. C. and Chiavérini, J.: Hydrological changes in the Ligurian Sea (NW
1083 Mediterranean, DYFAMED site) during 1995–2007 and biogeochemical consequences,
1084 Biogeosciences, 7, 2117–2128, https://doi.org/10.5194/bg-7-2117-2010, 2010.

1085 Mayot, N., D'Ortenzio, F., Ribera d'Alcalà, M., Lavigne, H., and Claustre, H.: Interannual
1086 variability of the Mediterranean trophic regimes from ocean color satellites,
1087 Biogeosciences, 13, 1901–1917, https://doi.org/10.5194/bg-13-1901-2016, 2016.

https://doi.org/10.5194/bg-2021-123
Preprint. Discussion started: 18 May 2021

1088 McClain, C. R., Signorini, S. R., and Christian, J. R.: Subtropical gyre variability observed by
1089 ocean-color satellites, Deep-Sea Res. Pt. II, 51, 281–301,
1090 https://doi.org/10.1016/j.dsr2.2003.08.002, 2004.

1091 McGillicuddy Jr., D. J.: Mechanisms of Physical-Biological-Biogeochemical Interaction at
1092 the Oceanic Mesoscale, Annu. Rev. Mar. Sci., 8–1, 125–159, 2016.

1093 Mignot, A., Claustre, H., Uitz, J., Poteau, A., D'Ortenzio, F., and Xing, X.: Understanding the
1094 seasonal dynamics of phytoplankton biomass and the deep chlorophyll maximum in
1095 oligotrophic environments: A Bio-Argo float investigation, Global Biogeochem. Cy.,
1096 28, 856– 876, https://doi.org/10.1002/2013GB004781, 2014.

1097 Minas, H. J.: La distribution de l'oxygène en relation avec la production primaire en
1098 Méditerranée Nord-Occidentale, Mar. Biol., 7, 181–204,
1099 https://doi.org/10.1007/BF00367489, 1970.

1100 Morel, A.: Light and marine photosynthesis: a spectral model with geochemical and
1101 climatological implications, Prog. Oceanogr., 26, 263–306,
1102 https://doi.org/10.1016/0079-6611(91)90004-6, 1991.

1103 Morel, A., and André, J.-M.: Pigment distribution and primary production in the western
1104 Mediterranean as derived and modeled from coastal zone color scanner observations, J.
1105 Geophys. Res., 96, 12685– 12698, https://doi.org/10.1029/91JC00788, 1991.

1106 Morel, A., Antoine, D., Babin, M., and Dandonneau, Y.: Measured and modeled primary
1107 production in the northeast Atlantic (EUMELI JGOFS program): the impact of natural
1108 variations in photosynthetic parameters on model predictive skill, Deep-Sea Res. Pt. I,
1109 43, 1273–1304, https://doi.org/10.1016/0079-6611(91)90004-6, 1996.

1110 Moutier, W., Duforêt-Gaurier, L., Thyssen, M., Loisel, H., Mériaux, X., Courcot, L.,
1111 Dessailly, D., Rêve, M.-H., Grégori, G., Alvain, S., Barani, A., Brutier, L., and

1112 Dugrnne, M.: Evolution of the scattering properties of phytoplankton cells from flow
1113 cytometry measurements, PLOS ONE, 12, e0181180,
1114 https://doi.org/10.1371/journal.pone.0181180, 2017.

1115 Neukermans, G., Loisel, H., Mériaux, X., Astoreca, R., and McKee, D.: In situ variability of
1116 mass-specific beam attenuation and backscattering of marine particles with respect to
1117 particle size, density, and composition, Limnol. Oceanogr., 57, 124–144,
1118 https://doi.org/10.4319/lo.2012.57.1.0124, 2012.

1119 Nielsen, E. S.: The Use of radio-active carbon (C^{14}) for measuring organic production in the
1120 sea, ICES J. Mar. Sci., 18, 117–140, https://doi.org/10.1093/icesjms/18.2.117, 1952.

1121 Organelli, E., Barbieux, M., Claustre, H., Schmechtig, C., Poteau, A., Bricaud, A., Boss, E.,
1122 Briggs, N., Dall'Olmo, G., D'Ortenzio, F., Leymarie, E., Mangin, A., Obolensky, G.,
1123 Penkerc'h, C., Prieur, L., Roesler, C., Serra, R., Uitz, J., and Xing, X.: Two databases
1124 derived from BGC-Argo float measurements for marine biogeochemical and bio-optical
1125 applications, Earth Syst. Sci. Data, 9, 861–880, https://doi.org/10.5194/essd-9-861-
1126 2017, 2017.

1127 Organelli, E., Dall'Olmo, G., Brewin, R. J. W., Taran, G., Boss, E., and Bricaud, A.: The
1128 open-ocean missing backscattering is in the structural complexity of particles, Nat.
1129 Commun., 9, 5439, https://doi.org/10.1038/s41467-018-07814-6, 2018.

1130 Oubelkheir, K., Claustre, H., Sciandra, A., and Babin, M.: Bio-optical and biogeochemical
1131 properties of different trophic regimes in oceanic waters, Limnol. Oceanogr., 50, 1795–
1132 1809, https://doi.org/10.4319/lo.2005.50.6.1795, 2015.

1133 Pasqueron de Fommervault, O., Migon, C., D'Ortenzio, F., Ribera d'Alcalà, M, and Coppola,
1134 L.: Temporal variability of nutrient concentrations in the northwestern Mediterranean

https://doi.org/10.5194/bg-2021-123
Preprint. Discussion started: 18 May 2021

1135 Sea (DYFAMED time-series station), Deep-Sea Res. Pt. I, 100, 1–12,
1136 https://doi.org/10.1016/j.dsr.2015.02.006, 2015.

1137 Polovina, J. J., Howell, E. A., and Abecassis, M.: Ocean's least productive waters are
1138 expanding, Geophys. Res. Lett., 35, L03618, https://doi.org/10.1029/2007GL031745,
1139 2008.

1140 Quay, P. D., Peacock, C., Björkman, K., and Karl, D. M.: Measuring primary production rates
1141 in the ocean: Enigmatic results between incubation and non-incubation methods at
1142 Station ALOHA, Glob. Biogeochem. Cy., 24, https://doi.org/10.1029/2009GB003665,
1143 2010.

1144 Ras, J., Claustre, H., and Uitz, J.: Spatial variability of phytoplankton pigment distributions in
1145 the Subtropical South Pacific Ocean: comparison between in situ and predicted data,
1146 Biogeosciences, 5, 353–369, https://doi.org/10.5194/bg-5-353-2008, 2008.

1147 Roesler, C. S. and Boss, E.: In Situ Measurement of the Inherent Optical Properties (IOPs)
1148 and Potential for Harmful Algal Bloom Detection and Coastal Ecosystem Observations.
1149 *In* Babin, M., Roesler, C. S. and Cullen, J. J., Real-time coastal observing systems for
1150 marine ecosystem dynamics and harmful algal blooms: Theory, instrumentation and
1151 modelling. UNESCO, 2008.

1152 Roesler, C., Uitz, J., Claustre, H., Boss, E., Xing, X., Organelli, E., Briggs, N., Bricaud, A.,
1153 Schmechtig, C., Poteau, A., D'Ortenzio, F., Ras, J., Drapeau, S., Haëntjens, N. and
1154 Barbieux, M.: Recommendations for obtaining unbiased chlorophyll estimates from in
1155 situ chlorophyll fluorometers: A global analysis of WET Labs ECO sensors, Limnol.
1156 Oceanogr.-Meth., 15, 572–585, https://doi.org/10.1002/lom3.10185, 2017.

https://doi.org/10.5194/bg-2021-123
Preprint. Discussion started: 18 May 2021

1157 Saba, V.S., Friedrichs, M. A. M., Carr, M.-E., et al.: Challenges of modeling depth-integrated
1158 marine primary productivity over multiple decades: A case study at BATS and HOT,
1159 Glob. Biogeochem. Cy., 24, doi: 10.1029/2009GB003655, 2010.

1160 Saba, V. S., Friedrichs, M. A. M., Antoine, D., Armstrong, R. A., Asanuma, I., Behrenfeld,
1161 M. J., Ciotti, A. M., Dowell, M., Hoepffner, N., Hyde, K. J. W., Ishizaka, J., Kameda,
1162 T., Marra, J., Mélin, F., Morel, A., O'Reilly, J., Scardi, M., Smith Jr., W. O., Smyth, T.
1163 J., Tang, S., Uitz, J., Waters, K., and Westberry, T. K.: An evaluation of ocean color
1164 model estimates of marine primary productivity in coastal and pelagic regions across
1165 the globe, Biogeosciences, 8, 489–503, https://doi.org/10.5194/bg-8-489-2011, 2011.

1166 Sarmiento, J. L., and Siegenthaler, U.: New production and the global carbon cycle, in:
1167 Primary productivity and biogeochemical cycles in the sea, Environmental Science
1168 Research, vol. 43, edited by Falkowski, P. G., Woodhead A. D., and Vivirito K.,
1169 Springer, Boston, MA, https://doi.org/10.1007/978-1-4899-0762-2_18, 1992.

1170 Sarmiento, J. L., Slater, R., Barber, R., Bopp, L., Doney, S. C., Hirst, A. C., Kleypas, J.,
1171 Matear, R., Mikolajewicz, U., Monfray, P., Soldatov, V., Spall, S. A., and Stouffer, R.:
1172 Response of ocean ecosystems to climate warming, Global Biogeochem. Cy., 18, 1–23,
1173 https://doi.org/10.1029/2003GB002134, 2014.

1174 Sathyendranath, S., Longhurst, A., Caverhill, C. M., and Platt, T.: Regionally and Seasonally
1175 Differentiated Primary Production in the North Atlantic, Deep-Sea Res. Pt. I, 42, 1773–
1176 1802, https://doi.org/10.1016/0967-0637(95)00059-F, 1995.

1177 Sathyendranath, S., Stuart, V., Nair, A., Oka, K., Nakane, T., Bouman, H., Forget, M.-H.,
1178 Maass, H., and Platt, T.: Carbon-to-chlorophyll ratio and growth rate of phytoplankton
1179 in the sea, Mar. Ecol. Prog. Ser., 383, 73–84, https://doi.org/10.3354/meps07998: 2009.

https://doi.org/10.5194/bg-2021-123
Preprint. Discussion started: 18 May 2021

1180 Schmechtig, C., Poteau, A., Claustre, H., D'Ortenzio, F., and Boss, E.: Processing Bio-Argo
1181 chlorophyll a concentration at the DAC Level, Argo Data Management, 1–22,
1182 https://doi.org/10.13155/39468, 2015.

1183 Schmechtig, C., Poteau, A., Claustre, H., D'Ortenzio, F., Dall'Olmo, G., and Boss, E.:
1184 Processing Bio-Argo particle backscattering at the DAC level Version, Argo Data
1185 Management, 1–13, https://doi.org/10.13155/39459, 2016.

1186 Serret, P., Fernandez, E., Sostres, J. A., and Anadon, R.: Seasonal compensation of microbial
1187 production and respiration in a temperate sea, Mar. Ecol. Prog. Ser., 187, 43–57,
1188 https://doi.org/10.3354/meps187043, 1999.

1189 Siegel, D. A., Dickey, T.D., Washburn, L., Hamilton, M. K., and Mitchell, B. G: Optical
1190 determination of particulate abundance and production variations in the oligotrophic
1191 ocean, Deep-Sea Res. Pt. A, 36, 211–222, https://doi.org/10.1016/0198-0149(89)90134-
1192 9, 1989.

1193 Signorini, S. R., Franz B. A., and McClain C. R.: Chlorophyll variability in the oligotrophic
1194 gyres: mechanisms, seasonality and trends, Frontiers Mar. Sci., 2,
1195 https://doi.org/10.3389/fmars.2015.00001, 2015.

1196 Siokou-Frangou, I., Christaki, U., Mazzocchi, M. G., Montresor, M., Ribera d'Alcalá, M.,
1197 Vaqué, D., and Zingone, A.: Plankton in the open Mediterranean Sea: a review,
1198 Biogeosciences, 7, 1543–1586, https://doi.org/10.5194/bg-7-1543-2010, 2010.

1199 Slade, W. H., and Boss, E.: Spectral attenuation and backscattering as indicators of average
1200 particle size, Applied Opt., 54, 7264–7277, http://dx.doi.org/10.1364/AO.54.007264,
1201 2015.

https://doi.org/10.5194/bg-2021-123
Preprint. Discussion started: 18 May 2021

1202 Stramska, M., and Dickey, T. D.: Variability of bio-optical properties of the upper ocean
1203 associated with diel cycles in phytoplankton population, J. Geophys. Res., 97, 17873–
1204 17887, https://doi.org/10.1029/92JC01570, 1992.

1205 Stramski, D., and Kiefer, D.A.: Light scattering by microorganisms in the open ocean. Prog.
1206 Oceanogr., 28, 343–383, https://doi.org/10.1016/0079-6611(91)90032-H, 1991.

1207 Stramski, D., and Reynolds, R. A.: Diel variations in the optical properties of a marine
1208 diatom. Limnol. Oceanogr., 38, 1347–1364, https://doi.org/10.4319/lo.1993.38.7.1347,
1209 1993.

1210 Stramski, D., Reynolds, R. A., Kahru, M., and Mitchell, B. G.: Estimation of particulate
1211 organic carbon in the ocean from satellite remote sensing, Science, 285, 239–242,
1212 https://doi.org/10.1126/science.285.5425.239, 1999.

1213 Stramski, D., Bricaud, A., and Morel, A.: Modeling the inherent optical properties of the
1214 ocean based on the detailed composition of the planktonic community, Appl. Opt., 40,
1215 2929–2945, https://doi.org/10.1364/AO.40.002929, 2001.

1216 Stramski, S., Boss, E., Bogucki, D., and Voss., K. J.: The role of seawater constituents in light
1217 backscattering in the ocean, Prog. Oceanogr., 61, 27–56,
1218 https://doi.org/10.1016/j.pocean.2004.07.001, 2004.

1219 Stramski, D., Reynolds, R. A., Babin, M., Kaczmarek, S., Lewis, M. R., Röttgers, R.,
1220 Sciandra, A., Stramska, M., Twardowski, M. S., Franz, B. A., and Claustre, H.:
1221 Relationships between the surface concentration of particulate organic carbon and
1222 optical properties in the eastern South Pacific and eastern Atlantic Oceans,
1223 Biogeosciences, 5, 171–201, https://doi.org/10.5194/bg-5-171-2008, 2008.

https://doi.org/10.5194/bg-2021-123
Preprint. Discussion started: 18 May 2021

1224 Sullivan, J., Twardowski, M., Ronald, S., Zaneveld, J. V., and Moore, C. C.: Measuring
1225 optical backscattering in water, in: Light scattering reviews, edited by Kokhanovsky, A.
1226 A., Springer, Berlin, 7, 189–224, 2013.

1227 Taillandier, V., Wagener, T., D'Ortenzio, F., Mayot, N., Legoff, H., Ras, J., Coppola, L.,
1228 Pasqueron de Fommervault, O., Schmechtig, C., Diamond, E., Bittig, H., Lefevre, D.,
1229 Leymarie, E., Poteau, A., and Prieur, L.: Hydrography and biogeochemistry dedicated
1230 to the Mediterranean BGC-Argo network during a cruise with RV Tethys 2 in May
1231 2015, Earth Syst. Sci. Data, 10, 627–641, https://doi.org/10.5194/essd-10-627-2018,
1232 2018.

1233 Turley, C. M., Bianchi, M., Christaki, U., Conan, P., Harris, J. R. W., Psarra, S., Ruddy, G.,
1234 Stutt, E. D., Tselepides, A., Van Wambeke, F.: Relationship between primary producers
1235 and bacteria in an oligotrophic sea - The Mediterranean and biogeochemical
1236 implications, Mar. Ecol. Progr. Ser., 193, 11–18, https://doi.org/10.3354/meps193011,
1237 2000.

1238 Twardowski, M. S., Boss, E., Macdonald, J. B., Pegau, W. S., Barnard, A. H., and Zaneveld,
1239 J. R. V.: A model for estimating bulk refractive index from the optical backscattering
1240 ratio and the implications for understanding particle composition in case I and case II
1241 waters. J. Geophys. Res., 106, 14129–14142, https://doi.org/10.1029/2000JC000404,
1242 2001.

1243 Uitz, J., Claustre, H., Morel, A., and Hooker, S. B.: Vertical distribution of phytoplankton
1244 communities in open ocean: An assessment based on surface chlorophyll, J. Geophys.
1245 Res., 111, 1–23, https://doi.org/10.1029/2005JC003207, 2006.

1246 Uitz, J., Claustre, H., Gentili, B., and Stramski, D.: Phyto- plankton class-specific primary
1247 production in the world's oceans: Seasonal and interannual variability from satellite

observations, Global Biogeochem. Cy., 24, 1–19, https://doi.org/10.1029/2009gb003680, 2010.

Uitz, J., Stramski, D., Gentili, B., D'Ortenzio, F., and Claustre, H.: Estimates of phytoplankton class-specific and total primary production in the Mediterranean Sea from satellite ocean color observations, Global Biogeochem. Cy., 26, 1–10, https://doi.org/10.1029/2011gb004055, 2012.

Ulloa, O., Sathyendranath, S., and Platt, T.: Effect of the particle-size distribution on the backscattering ratio in seawater, Appl. Opt., 33, 7070–7077, https://doi.org/10.1364/AO.33.007070, 1994.

Vaulot, D., and Marie, D.: Diel variability of photosynthetic picoplankton in the equatorial Pacific, J. Geophys. Res., 104, 3297–3310, https://doi.org/10.1029/98JC01333, 1999.

Vidussi, F., Claustre, H., Manca, B. B., Luchetta, A., and Marty, J.-C.: Phytoplankton pigment distribution in relation to upper thermocline circulation in the eastern Mediterranean Sea during winter, J. Geophys. Res., 106, 19,939-19,956, https://doi.org/10.1029/1999JC000308, 2001.

Westberry, T., Behrenfeld, M. J., Siegel, D. A., and Boss, E.: Carbon-based primary productivity modeling with vertically resolved photoacclimation, Global Biogeoch. Cy., 222, 1–18, https://doi.org/10.1029/2007GB003078, 2008.

Westberry, T. K. Dall'Olmo, G., Boss, E., Behrenfeld, M., and Moutin, T.: Coherence of particulate beam attenuation and backscattering coefficients in diverse open ocean environments, Opt. Express, 18, 15,419–15,425, https://doi.org/10.1364/OE.18.015419, 2010.

https://doi.org/10.5194/bg-2021-123
Preprint. Discussion started: 18 May 2021

1270 White, A. E., Barone, B., Letelier, R. M., and Karl, D. M.: Productivity diagnosed from the
1271 diel cycle of particulate carbon in the North Pacific Subtropical Gyre, Geophys. Res.
1272 Lett., 44, 3752– 3760, https://doi.org/10.1002/2016GL071607, 2017.

1273 Whitmire, A. L., Boss, E., Cowles, T. J., and Pegau, W. S.: Spectral variability of the
1274 particulate backscattering ratio, Opt. Express 15, 7019–7031,
1275 https://doi.org/10.1364/OE.15.007019, 2007.

1276 Williams, P. J. le B., and Jenkinson, N.W.: A transportable microprocessor controlled precise
1277 Winkler titration suitable for field station and shipboard use, Limnol. Oceanogr., 27,
1278 576–584, https://doi.org/10.4319/lo.1982.27.3.0576, 1982.

1279 Williams, P. J. le B., and Purdie, D. A.: In vitro and in situ derived rates of gross production,
1280 net community production and respiration of oxygen in the oligotrophic subtropical
1281 gyre of the North Pacific Ocean, Deep-Sea Res. Pt. A, 38, 891–910,
1282 https://doi.org/10.1016/0198-0149(91)90024-A, 1991.

1283 Williams, P. J. le B.: On the definition of plankton production terms, in: Measurement of
1284 primary production from the molecular to the global scale, edited by Li, W. K., and
1285 Maestrini, S. I., ICES mar. Sei. Symp, Copenhagen, 9–19, 1993.

1286 Williams, P. J. le B., Morris, P. J., and Karl, D. M.: Net community production and metabolic
1287 balance at the oligotrophic ocean site, station ALOHA, Deep-Sea Res. Pt. I, 51, 1563–
1288 1578, https://doi.org/10.1016/j.dsr.2004.07.001., 2004.

1289 Xing, X., Claustre, H., Blain, S., D'Ortenzio, F., Antoine, D., Ras, J., Guinet, C.: Quenching
1290 correction for in vivo chlorophyll fluorescence acquired by autonomous platforms: A
1291 case study with instrumented elephant seals in the Kerguelen region (Southern Ocean),
1292 Limnol. Oceanogr.-Meth., 10, 483–495, https://doi.org/10.4319/lom.2012.10.483, 2012.

https://doi.org/10.5194/bg-2021-123
Preprint. Discussion started: 18 May 2021

1293 Yentsch, C. S., and Phinney, D. A.: A bridge between ocean optics and microbial ecology.
1294 Limnol. Oceanogr., 34, 1694–1705, https://doi.org/10.4319/lo.1989.34.8.1694, 1989.
1295 Zhang, X., Hu, L., and He, M.-X.: Scattering by pure seawater: Effect of salinity, Opt.
1296 Express, 17, 5698–5710, https://doi.org/10.1364/OE.17.005698, 2009.

https://doi.org/10.5194/bg-2021-123
Preprint. Discussion started: 18 May 2021

Figure captions

Figure 1: Trajectories of the two BGC-Argo profiling floats fLig (WMO6901776) and fIon (WMO6902828) deployed respectively in the Ligurian Sea (green) and the Ionian Sea (blue).

Figure 2: Schematic representation of the diel variations of the depth-integrated bio-optical properties converted to POC biomass (B) and the sampling strategies employed in the (a) Ligurian Sea and (b) Ionian Sea. The diamond-shaped symbols indicate schematically the float profile times, labeled with time stamps associated with sunrise (sr), noon (n), sunset (ss) and midnight (m), with the corresponding POC biomass estimated within the considered layer (e.g., $B(t_{sr})$, etc.). The numeric subscripts (+1, +2, +4 or +5) indicate the number of days since the first profile of the summertime time series.

Figure 3: Time series of Chl (a and d), b_{bp} (b and e) and c_p (d and f) in the Ligurian Sea (left) and the Ionian Sea (right). The Mixed Layer Depth (MLD; black line), the isopycnal 28.85, expressed as σ_t (blue line), the euphotic depth (Z_{eu}; white line) and the depth of the SCM (magenta line) are superimposed onto the bio-optical timeseries. The dashed lines indicate the dates at which the c_p and the b_{bp} values in the SCM layer reach a minimum.

Figure 4: Temporal evolution of Chl (a and d), c_{bp} (b and e), and b_{bp} (c and f) in the surface (red) and SCM (dark green) layers for the Ligurian Sea (left) and the Ionian Sea (right). The dashed lines indicate the dates when the values of c_p and b_{bp} in the SCM layer reach a minimum

Figure 5: Example of the variations of the c_p (a) and b_{bp} (b) coefficients at the daily time scale in the Ionian Sea in the SCM layer during the interval from September 2 to September 6, 2017. The grey shaded area indicates the nighttime.

Figure 6: Comparison of the biological production integrated within the euphotic layer, derived from the diel cycle of c_p (blue) or b_{bp} (yellow) or computed using the bio-optical primary production model of Morel (1991) (purple) for the Ligurian Sea (a) and the Ionian Sea (b).

Figure 7: Temporal evolution of the POC and community production derived from the diel cycle of c_p in the Ligurian Sea (a– b) and the Ionian Sea (c–d) and integrated in three different layers of the water column: surface (dark green), euphotic (light blue) and SCM (red) layers. The dotted lines indicate the dates when c_p in the SCM layer reaches a minimum.

https://doi.org/10.5194/bg-2021-123
Preprint. Discussion started: 18 May 2021

Figure 8: Depth-interpolated time series of the relative contributions to the chlorophyll *a* concentration (%) of the micro- (a and d), nano- (b and e) and picophytoplankton (c and h) derived from HPLC pigment determinations in the Ligurian Sea (BOUSSOLE site; left) and the Ionian Sea (PEACETIME cruise; right). The pigment data were collected at the BOUSSOLE site in the same region and at the same time period as the fLig float deployment on May 24, 2014 (see text section 2.1). The fION float was deployed concurrently to sampling for HPLC pigments at the PEACETIME ION station on May 28, 2017. Pigment data collected at ION over four days prior to float deployment are shown.

Figure 9: Temporal evolution of the bio-optical ratios of b_{bp} / c_p (a), c_p / Chl (b) and b_{bp} / Chl (c) in the SCM layer for the Ligurian Sea (left) and the Ionian Sea (right). The dotted lines indicate the dates when the values of c_p in the SCM layer reach a minimum.

Figure 10: Time series of the daily-integrated photosynthetically available radiation (PAR) at the SCM level in the Ligurian Sea (a) and the Ionian Sea (b). The horizontal grey line shows the median of each time series. The dotted lines indicate the dates at which the values of c_p in the SCM layer reach a minimum.

https://doi.org/10.5194/bg-2021-123
Preprint. Discussion started: 18 May 2021

Table 1: POC-to-c_p relationships from the literature, with POC and c_p in units of mg m^{-3} and m^{-1}, respectively.

Reference	Region	Relationship
Marra et al. (1995)	North Atlantic	POC = 367 $c_p(660)$ + 31.2
Claustre et al. (1999)	Equatorial Pacific	POC = 501.81 $c_p(660)$ + 5.33
Oubelkheir et al. (2005)	Mediterranean	POC = 574 $c_p(555)$ – 7.4
Behrenfeld & Boss (2006)	Equatorial Pacific	POC = 585.2 $c_p(660)$ + 7.6
Gardner et al. (2006)	Global Ocean	POC = 381 $c_p(660)$ + 9.4
Stramski et al. (2008)	Pacific and Atlantic, including upwelling	POC = 661.9 $c_p(660)$ – 2.168
Loisel et al (2011)	Mediterranean	POC = 404 $c_{bp}(660)$ + 29.25
Cetinić et al. (2012)	North Atlantic	POC = 391 $c_p(660)$ – 5.8

https://doi.org/10.5194/bg-2021-123
Preprint. Discussion started: 18 May 2021

Table 2: POC-to-b_{bp} relationships from the literature, with POC and b_{bp} in units of mg m^{-3} and m^{-1}, respectively.

Reference	Region	Relationship
Stramski et al. (2008)	Pacific and Atlantic, including upwelling	POC = 71002 $b_{bp}(555)$ –5.5
Loisel et al (2011)	Mediterranean	POC = 37550 $b_{bp}(555)$ + 1.3
Cetinić et al. (2012)	North Atlantic	POC = 35422 $b_{bp}(700)$ – 14.4

https://doi.org/10.5194/bg-2021-123
Preprint. Discussion started: 18 May 2021

Table 3: Mean and range (%) in relative daily variations ($\widetilde{\mathbf{m}}\tilde{\Delta}$ and $\widetilde{\mathbf{r}}\tilde{\Delta}$, respectively) in the diel cycle of c_p and b_{bp} computed for each float over the entire time series, for the two considered regions and in the different layers of the water column, i.e. surface (0-Z_{pd}), SCM (SCM), and euphotic (0-Z_{eu}) layers.

		Surface layer		SCM layer		Euphotic layer	
Region		$\tilde{\Delta}\mathbf{c_p}$	$\tilde{\Delta}\mathbf{b_{bp}}$	$\tilde{\Delta}\mathbf{c_p}$	$\tilde{\Delta}\mathbf{b_{bp}}$	$\tilde{\Delta}\mathbf{c_p}$	$\tilde{\Delta}\mathbf{b_{bp}}$
Ligurian Sea	$\widetilde{\mathbf{m}}\tilde{\Delta}$	12.7	-2.3	14.5	3.8	-134.9	1.1
	$\widetilde{\mathbf{r}}\tilde{\Delta}$	256.7	28.5	194.8	107.8	2603.1	20.5
Ionian Sea	$\widetilde{\mathbf{m}}\tilde{\Delta}$	0.55	0.23	1.16	0.06	0.39	0.21
	$\widetilde{\mathbf{r}}\tilde{\Delta}$	54.4	21.2	102.4	57.3	55.9	24.9

https://doi.org/10.5194/bg-2021-123
Preprint. Discussion started: 18 May 2021

Table 4: Estimates of primary and community production (in units of gC m^{-2} d^{-1}) from the literature in areas of the Mediterranean Sea comparable, when possible, to the considered study regions.

Primary production					
Method	**Reference**	**Area**	**Period**	**Layer**	**Estimate**
Ocean color-coupled bio-optical model	Morel & André (1991)	Western basin	1981	0-Z_{eu}	0.26
	Antoine et al. (1995)	Whole basin	1979-1981	0-1.5Z_{eu}	0.34
	Bosc et al. (2004)	Western basin	1998-2001	0-1.5Z_{eu}	0.45
	-	Eastern basin	-	-	0.33
	Uitz et al. (2012)	Bloom region	May-Aug 1998-2007	0-1.5Z_{eu}	0.26–0.82
	-	No blom region	-	-	0.22–0.69
Biogeochemical model	Lacroix & Nival (1998)	Ligurian Sea		0-200 m	0.13
	Allen et al. (2002)	Ligurian Sea		0-Z_{eu}	0.33
	-	Ionian Sea		-	0.14
In-situ ^{14}C measurements	Minas (1970)	Northwestern basin	1961-1965	Surface	0.21
	Magazzu & Decembrini (1995)	Ionian Sea	1983-1992	0-Z_{eu}	0.22
	Turley et al. (2000)	Ligurian Sea	Oct 1997, Apr-May 1998	0-Z_{eu}	0.5
	Marañon et al. (2021)	Ionian Sea	May 2017	0-200 m	0.19

Gross community production					
Method	**Reference**	**Area**	**Period**	**Layer**	**Estimate**
c_p diel cycle-based method	Barnes & Antoine (2014)	Ligurian Sea	May-Aug 2006-2011	0-Z_{eu}	0.8-1.5

https://doi.org/10.5194/bg-2021-123
Preprint. Discussion started: 18 May 2021

Table 5: Comparison of the mean rates ± SD (gC m^{-2} d^{-1}) of the community production integrated within the euphotic layer, derived from the application of the bio-optical diel cycle-based method to the c_p measurements, using different bio-optical relationships from the literature for converting the c_p values into POC biomass.

Reference	Ligurian Sea	Ionian Sea
Marra et al. (1995)	0.89±0.84	0.35±0.09
Claustre et al. (1999)	1.22±1.16	0.48±0.12
Oubelkheir et al. (2005)	1.18±1.13	0.46±0.11
Behrenfeld & Boss (2006)	1.43±1.35	0.56±0.14
Gardner et al. (2006)	0.93±0.88	0.36±0.09
Stramski et al. (2008)	1.62±1.54	0.63±0.16
Loisel et al. (2011)	0.98±0.92	0.38±0.10
Cetinić et al. (2012)	0.96±0.91	0.37±0.09

https://doi.org/10.5194/bg-2021-123
Preprint. Discussion started: 18 May 2021

Table 6: Community production mean rates ± SD (gC m^{-2} d^{-1}) derived from the application of the bio-optical diel cycle-based method to the c_p measurements in the two considered regions. The production rates are integrated within the surface, subsurface maximum, and euphotic layers.

Variable	Ligurian Sea			Ionian Sea		
	Euphotic	Surface	SCM	Euphotic	Surface	SCM
POC (gC m^{-2} d^{-1})	3.67±1.11	0.36±0.17	3.86 ± 1.20	1.88 ±0.24	0.34±0.14	0.93±0.31
GCP (gC m^{-2} d^{-1})	1.18±1.13	0.29±0.33	0.96±1.28	0.46±0.11	0.11±0.04	0.14± 0.39

https://doi.org/10.5194/bg-2021-123
Preprint. Discussion started: 18 May 2021

Biogeosciences
Discussions
Open Access
EGU

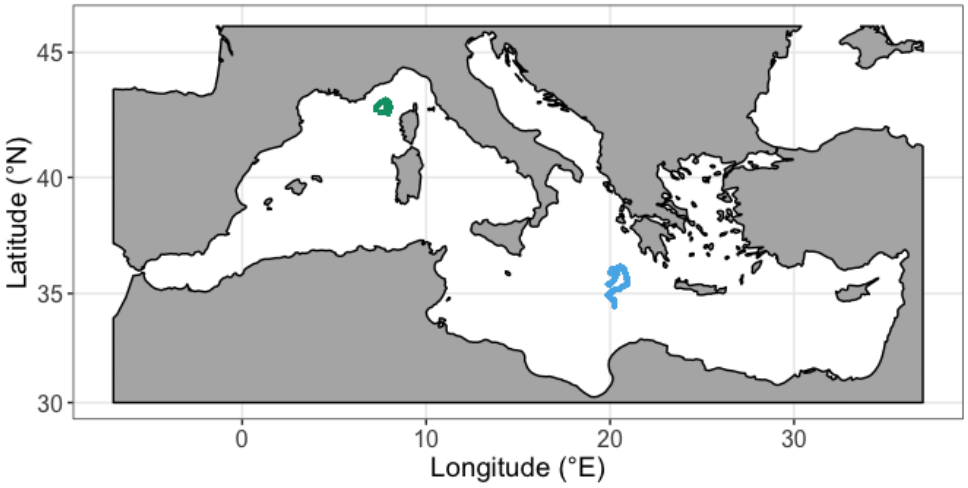

Figure 1: Trajectories of the two BGC-Argo profiling floats fLig (WMO6901776) and fIon (WMO6902828) deployed respectively in the Ligurian Sea (green) and the Ionian Sea (blue).

https://doi.org/10.5194/bg-2021-123
Preprint. Discussion started: 18 May 2021

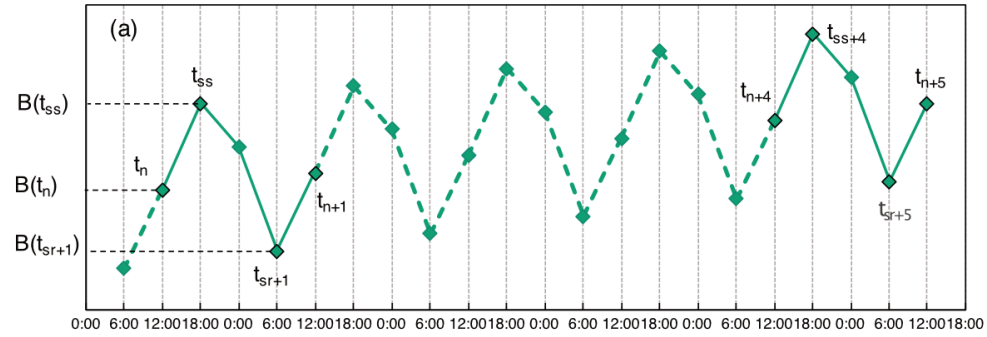

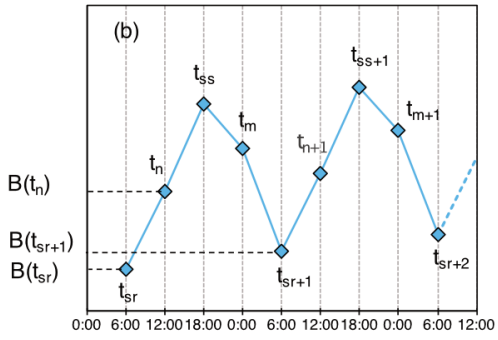

Figure 2: Schematic representation of the diel variations of the depth-integrated bio-optical properties converted to POC biomass (B) and the sampling strategies employed in the (a) Ligurian Sea and (b) Ionian Sea. The diamond-shaped symbols indicate schematically the float profile times, labeled with time stamps associated with sunrise (sr), noon (n), sunset (ss) and midnight (m), with the corresponding POC biomass estimated within the considered layer (e.g., $B(t_{sr})$, etc.). The numeric subscripts (+1, +2, +4 or +5) indicate the number of days since the first profile of the summertime time series.

https://doi.org/10.5194/bg-2021-123
Preprint. Discussion started: 18 May 2021

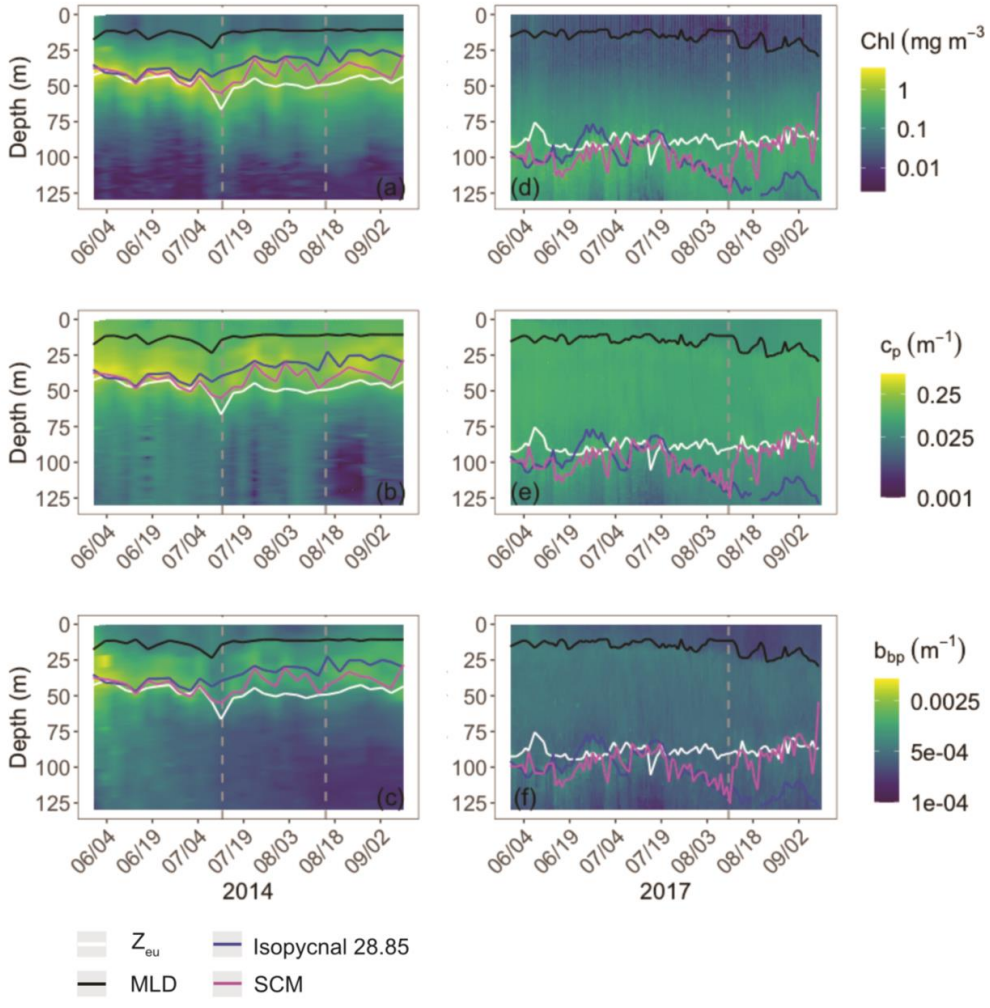

Figure 3: Time series of Chl (a and d), b_{bp} (b and e) and c_p (d and f) in the Ligurian Sea (left) and the Ionian Sea (right). The Mixed Layer Depth (MLD; black line), the isopycnal 28.85, expressed as σ_t (blue line), the euphotic depth (Z_{eu}; white line) and the depth of the SCM (magenta line) are superimposed onto the bio-optical timeseries. The dashed lines indicate the dates at which the c_p and the b_{bp} values in the SCM layer reach a minimum.

https://doi.org/10.5194/bg-2021-123
Preprint. Discussion started: 18 May 2021

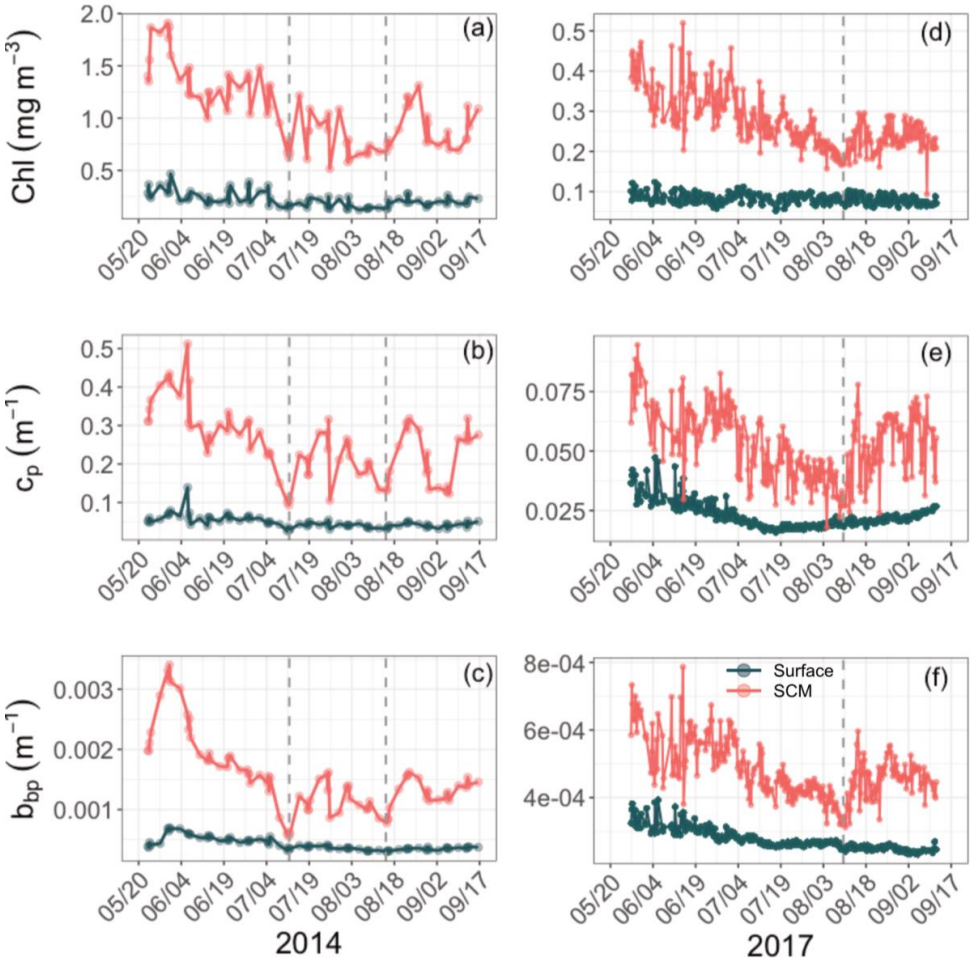

Figure 4: Temporal evolution of Chl (a and d), c_{bp} (b and e), and b_{bp} (c and f) in the surface (red) and SCM (dark green) layers for the Ligurian Sea (left) and the Ionian Sea (right). The dashed lines indicate the dates when the values of c_p and b_{bp} in the SCM layer reach a minimum.

https://doi.org/10.5194/bg-2021-123
Preprint. Discussion started: 18 May 2021

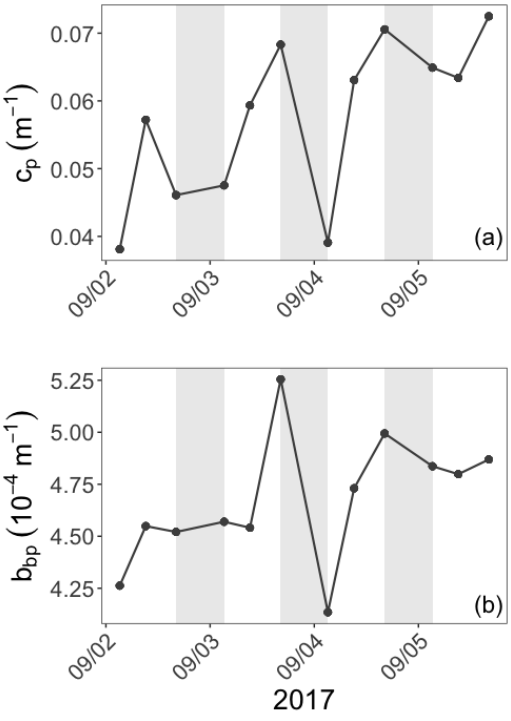

Figure 5: Example of the variations of the c_p (a) and b_{bp} (b) coefficients at the daily time scale in the Ionian Sea in the SCM layer during the interval from September 2 to September 6, 2017. The grey shaded area indicates the nighttime.

https://doi.org/10.5194/bg-2021-123
Preprint. Discussion started: 18 May 2021

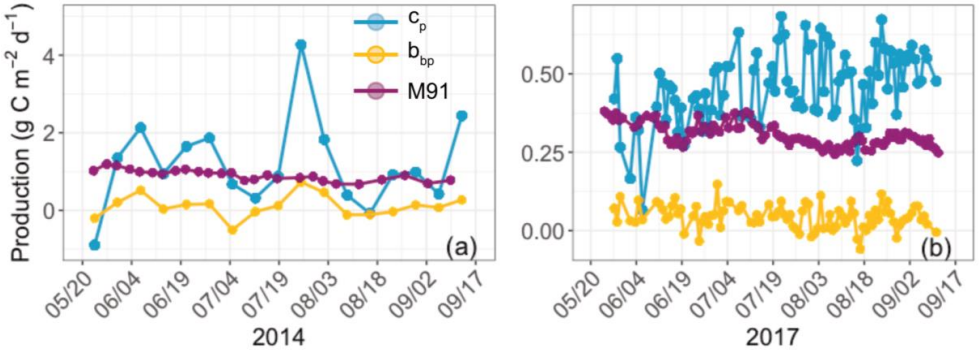

Figure 6: Comparison of the biological production integrated within the euphotic layer, derived from the diel cycle of c_p (blue) or b_{bp} (yellow) or computed using the bio-optical primary production model of Morel (1991) (purple) for the Ligurian Sea (a) and the Ionian Sea (b).

https://doi.org/10.5194/bg-2021-123
Preprint. Discussion started: 18 May 2021

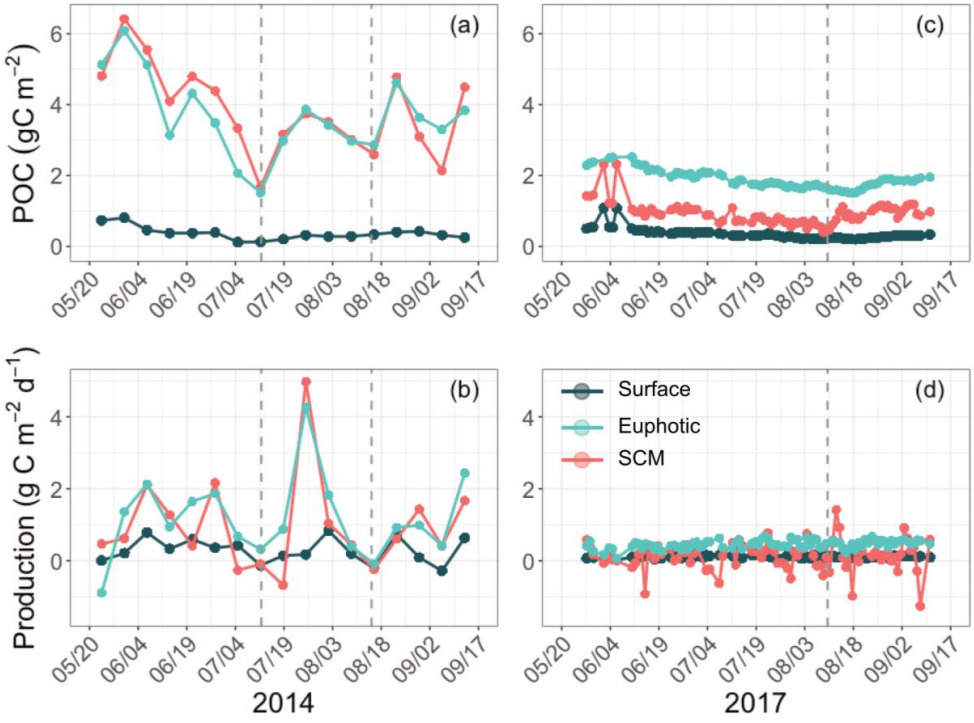

Figure 7: Temporal evolution of the POC and community production derived from the diel cycle of c_p in the Ligurian Sea (a– b) and the Ionian Sea (c–d) and integrated in three different layers of the water column: surface (dark green), euphotic (light blue) and SCM (red) layers. The dotted lines indicate the dates when c_p in the SCM layer reaches a minimum.

https://doi.org/10.5194/bg-2021-123
Preprint. Discussion started: 18 May 2021

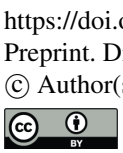

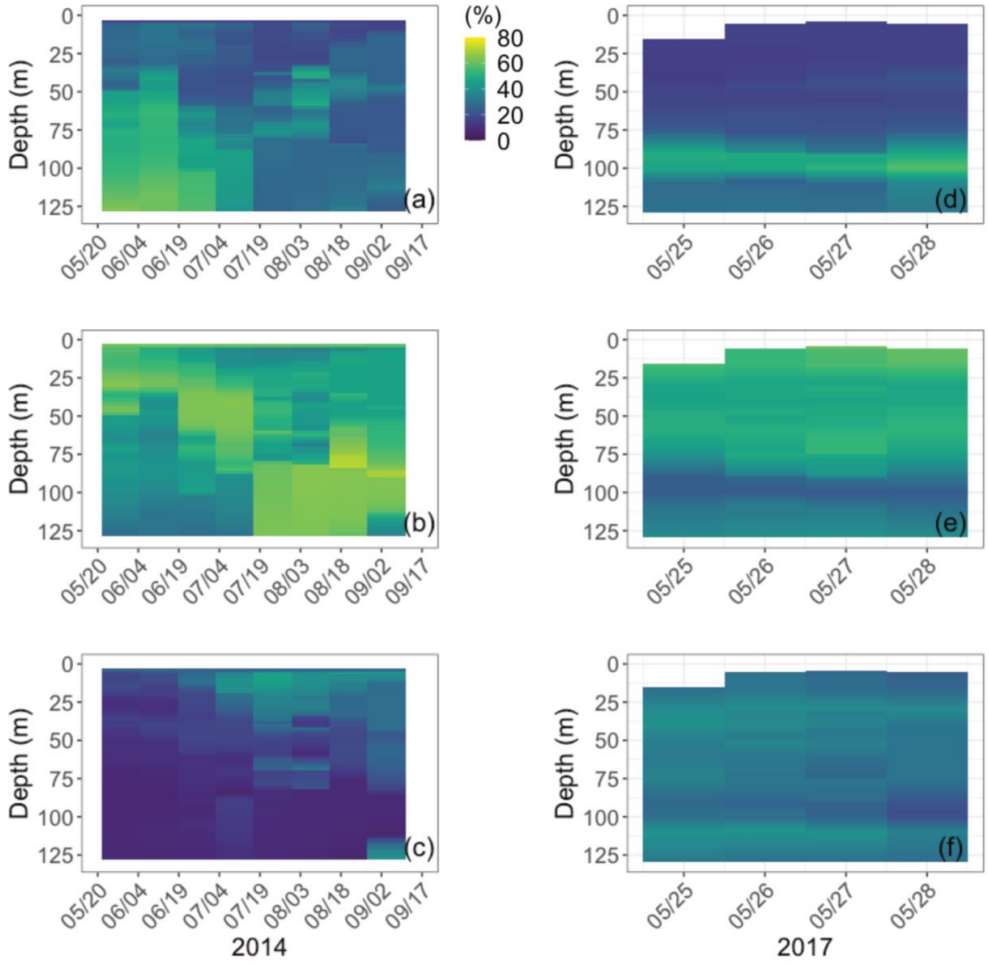

Figure 8: Depth-interpolated time series of the relative contributions to the chlorophyll *a* concentration (%) of the micro- (a and d), nano- (b and e) and picophytoplankton (c and h) derived from HPLC pigment determinations in the Ligurian Sea (BOUSSOLE site; left) and the Ionian Sea (PEACETIME cruise; right). The pigment data were collected at the BOUSSOLE site in the same region and at the same time period as the fLig float deployment on May 24, 2014 (see text section 2.1). The fION float was deployed concurrently to sampling for HPLC pigments at the PEACETIME ION station on May 28, 2017. Pigment data collected at ION over four days prior to float deployment are shown.

https://doi.org/10.5194/bg-2021-123
Preprint. Discussion started: 18 May 2021

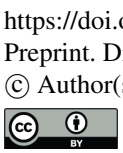

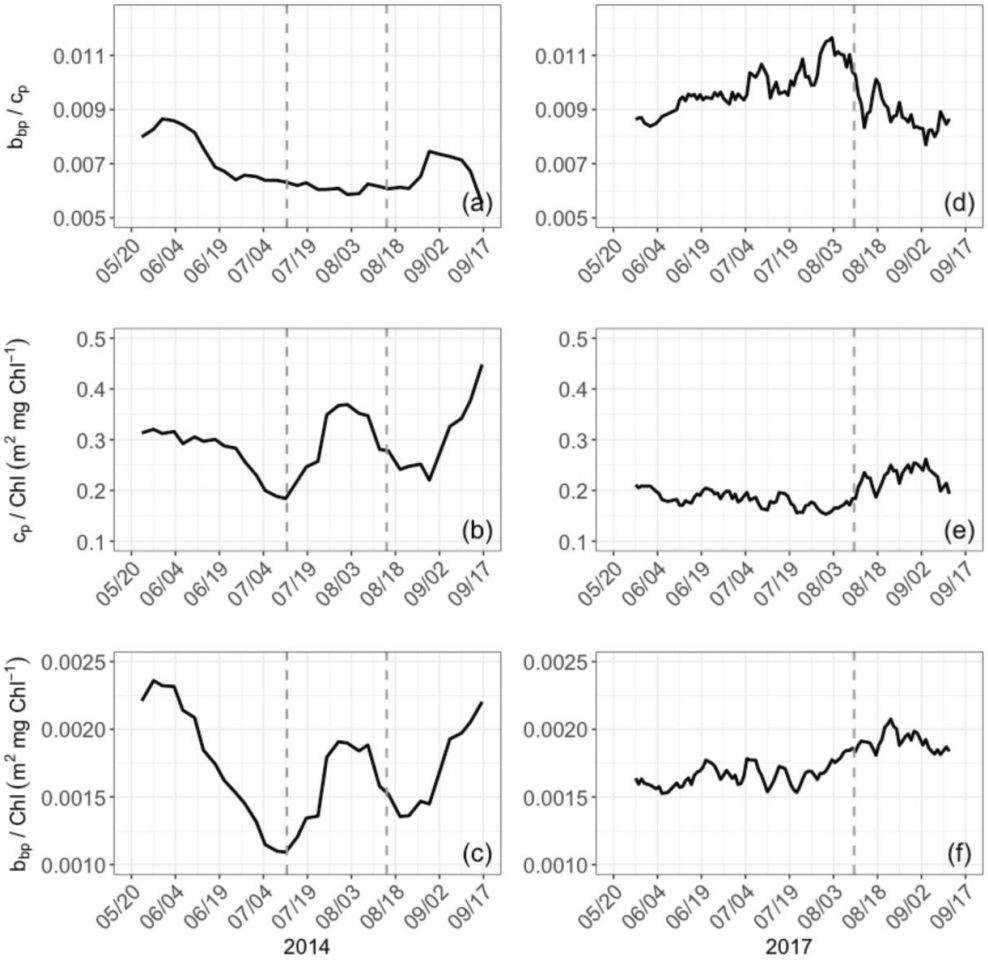

Figure 9: Temporal evolution of the bio-optical ratios of b_{bp} / c_p (a), c_p / Chl (b) and b_{bp} / Chl (c) in the SCM layer for the Ligurian Sea (left) and the Ionian Sea (right). The dotted lines indicate the dates when the values of c_p in the SCM layer reach a minimum.

https://doi.org/10.5194/bg-2021-123
Preprint. Discussion started: 18 May 2021

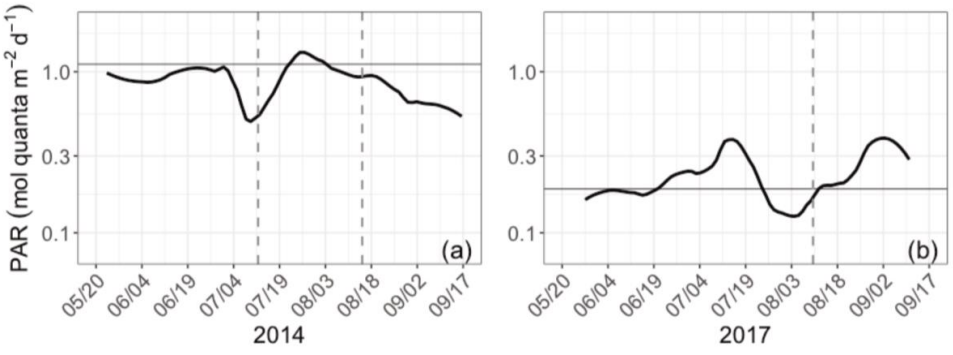

Figure 10: Time series of the daily-integrated photosynthetically available radiation (PAR) at the SCM level in the Ligurian Sea (a) and the Ionian Sea (b). The horizontal grey line shows the median of each time series. The dotted lines indicate the dates at which the values of c_p in the SCM layer reach a minimum.